MOLECULAR AND CELLULAR BIOLOGY, Aug. 1999, p. 5659–5674 Vol. 19, No. 8
0270-7306/99/$04.00+0

Bcl-2 and Bcl-X_L Block Thapsigargin-Induced Nitric Oxide Generation, c-Jun NH_2-Terminal Kinase Activity, and Apoptosis

RAKESH K. SRIVASTAVA,[1]* STEVEN J. SOLLOTT,[2] LEILA KHAN,[1] RICHARD HANSFORD,[3] EDWARD G. LAKATTA,[2] AND DAN L. LONGO[1]

Laboratory of Immunology,[1] Laboratory of Cardiovascular Sciences,[2] and Laboratory of Molecular Genetics,[3] Intramural Research Program, National Institute on Aging, National Institutes of Health, Baltimore, Maryland 21224-6825

Received 31 August 1998/Returned for modification 27 October 1998/Accepted 29 April 1999

The proteins Bcl-2 and Bcl-X_L prevent apoptosis, but their mechanism of action is unclear. We examined the role of Bcl-2 and Bcl-X_L in the regulation of cytosolic Ca^{2+}, nitric oxide production (NO), c-Jun NH_2-terminal kinase (JNK) activation, and apoptosis in Jurkat T cells. Thapsigargin (TG), an inhibitor of the endoplasmic reticulum-associated Ca^{2+} ATPase, was used to disrupt Ca^{2+} homeostasis. TG acutely elevated intracellular free Ca^{2+} and mitochondrial Ca^{2+} levels and induced NO production and apoptosis in Jurkat cells transfected with vector (JT/Neo). Buffering of this Ca^{2+} response with 1,2-bis(*o*-aminophenoxy)ethane-*N*,*N*,*N*′,*N*′-tetraacetic acid tetra(acetoxymethyl) ester (BAPTA-AM) or inhibiting NO synthase activity with N^G-nitro-L-arginine methyl ester hydrochloride (L-NAME) blocked TG-induced NO production and apoptosis in JT/Neo cells. By contrast, while TG produced comparable early changes in the Ca^{2+} level (i.e., within 3 h) in Jurkat cells overexpressing Bcl-2 and Bcl-X_L (JT/Bcl-2 or JT/Bcl-X_L), NO production, late (36-h) Ca^{2+} accumulation, and apoptosis were dramatically reduced compared to those in JT/Neo cells. Exposure of JT/Bcl-2 and JT/Bcl-X_L cells to the NO donor, *S*-nitroso-*N*-acetylpenacillamine (SNAP) resulted in apoptosis comparable to that seen in JT/Neo cells. TG also activated the JNK pathway, which was blocked by L-NAME. Transient expression of a dominant negative mutant SEK1 (Lys→Arg), an upstream kinase of JNK, prevented both TG-induced JNK activation and apoptosis. A dominant negative c-Jun mutant also reduced TG-induced apoptosis. Overexpression of Bcl-2 or Bcl-X_L inhibited TG-induced loss in mitochondrial membrane potential, release of cytochrome *c*, and activation of caspase-3 and JNK. Inhibition of caspase-3 activation blocked TG-induced JNK activation, suggesting that JNK activation occurred downstream of caspase-3. Thus, TG-induced Ca^{2+} release leads to NO generation followed by mitochondrial changes including cytochrome *c* release and caspase-3 activation. Caspase-3 activation leads to activation of the JNK pathway and apoptosis. In summary, Ca^{2+}-dependent activation of NO production mediates apoptosis after TG exposure in JT/Neo cells. JT/Bcl-2 and JT/Bcl-X_L cells are susceptible to NO-mediated apoptosis, but Bcl-2 and Bcl-X_L protect the cells against TG-induced apoptosis by negatively regulating Ca^{2+}-sensitive NO synthase activity or expression.

Apoptosis (programmed cell death) is an important physiological process, and when dysregulated, it contributes to the pathogenesis of a variety of diseases including cancer, autoimmunity, and neurodegenerative disorders (22, 61). Apoptosis results from the action of a genetically encoded suicide program that leads to a series of characteristic morphological and biochemical changes (22, 60, 70). These changes include activation of caspases, mitochondrial depolarization, loss of cell volume, chromatin condensation, and nucleosomal DNA fragmentation (10, 22, 60, 70). Among the growing number of genes that are understood to regulate apoptosis is the Bcl-2 family of genes (5, 51, 53). Some of the proteins within this family, including Bcl-2 and Bcl-X_L, inhibit apoptosis, and others, such as Bax and Bak, promote apoptosis and in some instances are sufficient to cause apoptosis independent of additional signals (49, 51, 53). Bcl-2 and related antiapoptotic proteins appear to act in part by dimerizing with a proapoptotic molecule (e.g., Bax) and interfering with the apoptosis induced by Bax (45, 58).

Several different biochemical changes have been proposed to be the essential event that commits a cell to undergo apoptosis (46–53). These events include the generation of reactive oxygen species (ROS), induction of nitric oxide synthase (NOS), increase in the intracellular calcium level, loss of mitochondrial membrane potential, cytochrome *c* redistribution, and caspase activation (20, 48, 50, 51, 62, 70). All of these biochemical perturbations can result from alterations in mitochondrial function (50, 53, 70). In addition, at least two resident mitochondrial proteins, apoptosis-initiating factor (AIF) and cytochrome *c*, have been implicated in the activation of caspases (34, 52, 59).

It has been shown that Bcl-2 and Bcl-X_L may regulate ion fluxes (2, 19, 31, 32, 37, 38). This concept is supported by evidence that Bcl-2 overexpression decreases Ca^{2+} efflux through the endoplasmic reticulum (ER) membrane following thapsigargin (TG) treatment (19), prevents Ca^{2+} redistribution from the ER into the mitochondria following growth factor withdrawal (2), and inhibits apoptosis-associated Ca^{2+} waves (31, 37) and nuclear Ca^{2+} uptake (38). Bcl-2 overexpression also enhances the uptake of calcium by mitochondria (42, 56) and preserves mitochondrial transmembrane potential (71). These findings suggest that Bcl-2 might act as a regulator of intracellular Ca^{2+} concentration through its interaction with the ER and mitochondrial membranes. However, it has been hypothesized that Bcl-2 may heterodimerize with Bax and form pores, similar to those made by bacterial toxins, which can function as channels in the ER and mitochondrial membranes

* Corresponding author. Mailing address: Laboratory of Immunology, National Institute on Aging, National Institutes of Health, 5600 Nathan Shock Dr., Box 9, Baltimore, MD 21224-6825. Phone: (410) 558-8110. Fax: (410) 558-8137. E-mail: longod@vax.grc.nia.nih.gov.

for ions, proteins, or both (50, 51). With Bcl-2 inducing the closing and Bax stimulating the opening of the pores, the ratio of Bcl-2 to Bax may determine the concentration of Ca^{2+} released into the cytoplasm (50, 51). Recent findings provide strong evidence that Bcl-X_L also regulates ion fluxes. First, the X-ray and nuclear magnetic resonance spectroscopy structure of Bcl-X_L resembles the physical structure of ion channel-forming bacterial toxins (41). Second, Bcl-X_L forms an ion channel in synthetic lipid membranes (33, 40). It has been shown that Bcl-X_L forms a cation-selective channel that conducts sodium but not calcium (31).

Recent evidence suggests that the JNK/SAPK pathway may play an important role in triggering apoptosis in response to inflammatory cytokines (interleukin-1, tumor necrosis factor alpha), free radicals generated by UV and gamma radiation, or direct application of H_2O_2 (7, 11, 12, 30, 35, 36, 67). In response to the above cellular stresses, JNK is strongly activated (11, 12). Overexpression of dominant negative mutants of components in the JNK pathway, such as ASK1(K709R), SEK1(Lys→Arg) (both are upstream kinases), and c-JunΔ169 (a downstream target), can effectively prevent apoptosis (18, 25, 67, 69). Furthermore, transfection of the constitutively activated forms of ASK1, SEK1, or c-Jun results in apoptotic cell death (18, 25, 67, 69).

In the present study, we used TG, an ER Ca^{2+}-ATPase inhibitor, to disrupt calcium homeostasis. The objectives of this study were to investigate (i) the effect of Bcl-2 and Bcl-X_L overexpression on TG-induced intracellular Ca^{2+} accumulation in Jurkat T lymphocytes and (ii) the intracellular mechanisms mediating TG-induced apoptosis in Jurkat T lymphocytes. Our results indicate that TG-induced apoptosis results from a transient increase of intracellular free calcium levels, calcium-dependent nitric oxide production, cytochrome *c* redistribution, reduction in mitochondrial membrane potential ($\Delta\Psi_m$), and activation of caspase-3 and the JNK pathway. Overexpression of Bcl-2 and Bcl-X_L antagonizes apoptosis early in this pathway by blocking the capacity of cells to generate nitric oxide.

MATERIALS AND METHODS

Reagents. TG and 4′,6-diamidino-2-phenylindole (DAPI) were purchased from Sigma Chemical Co. (St. Louis, Mo.). EGTA, SNAP, 1,2-bis(*o*-aminophenoxy)ethane-*N*,*N*,*N*′,*N*′-tetraacetic acid tetra(acetoxymethyl)ester (BAPTA-AM), cyclopiazonic acid (CPA), and PD098059 were purchased from Calbiochem (La Jolla, Calif.). Antibody against Bcl-2 was purchased from Oncogene Science (Uniondale, N.Y.). Antibodies against JNK1, ERK2, and p38 were purchased from Santa Cruz Biotechnology Inc. (Santa Cruz, Calif.). Antibodies against phospho-specific SAPK/JNK, extracellular signal-related kinase (ERK), and p38 were purchased from New England Biolabs, Inc. (Beverly, Mass.). Carbonyl cyanide-*p*-trifluoromethoxyphenylhydrazone (FCCP), indo-1/AM,3,3′-dihexyloxacarbocyanine iodide [$DiOC_6(3)$], N^G-nitro-L-arginine methyl ester hydrochloride (L-NAME), N^G-methyl-D-arginine acetate salt (D-NMMA), rhod-2, Mito Tracker Green FM, and anti-cytochrome oxidase (subunit IV) antibody were purchased from Molecular Probes, Inc. (Eugene, Oreg.). Anti-cytochrome *c* antibody was purchased from Pharmingen (San Diego, Calif.). The apoptosis detection kit (annexin V-fluorescein and propidium iodide) was purchased from R & D Systems (Minneapolis, Minn.). Anti-Flag M2 antibody was purchased from Kodak (Rochester, N.Y.). [γ-^{32}P]ATP (specific activity, 3,000 Ci/mmol) was purchased from ICN Pharmaceuticals, Inc. (Irvine, Calif.). The caspase inhibitors z-DEVD-fmk (CBZ-Asp-Glu-Val-Asp-fluoromethylketone) and z-VAD-fmk (CBZ-Val-Ala-Asp-fluoromethylketone) were purchased from Enzyme Systems Products (Livermore, Calif.). Enhanced chemiluminescence Western blot detection reagents were purchased from Amersham Life Sciences Inc. (Arlington Heights, Ill.). Dominant negative SEK1 (Lys→Arg) and glutathione *S*-transferase (GST)–c-Jun vectors were provided by J. Kyriakis (Massachusetts General Hospital, Charlestown, Mass.); pCDFLAGΔ169 DNA was from J. Ham (University College London, London, United Kingdom). The protein concentration was measured with the Micro BCA kit (Pierce, Rockford, Ill.). The nucleosome enzyme-linked immunosorbent assay (ELISA) kit was purchased from Oncogene Research Products (Cambridge, Mass.). The caspase-3 assay kit was purchased from Clontech Laboratories, Inc. (Palo Alto, Calif.).

Cells and culture conditions. Jurkat T cells were obtained from the American Type Culture Collection (Rockville, Md.). The cells were cultured at 37°C under 5% CO_2 in RPMI 1640 tissue culture medium (Bio Whittaker Inc., Walkersville, Md.) supplemented with 2 mM L-glutamine, 10% fetal bovine serum, and 1% penicillin-streptomycin mixture. The concentration of calcium in RPMI 1640 medium was 1.4 mM. For short-wavelength UV light (UVC) treatment of cells, the medium was removed and the cells were washed twice with phosphate-buffered saline. The cells were irradiated at a dose rate of 20 or 40 J/m^2 (as described in the figure legends), after which the original culture medium was added back to the cells.

Transfection of Bcl-2 and Bcl-X_L genes. Jurkat T lymphocytes (2×10^6) were transfected with pSFFVneo–Bcl-2, pSFFVneo–Bcl-X_L or pSFFV-neo (a gift from Stanley Korsmeyer, Dana-Farber Cancer Institute, Boston, Mass.) with Lipofectin (GIBCO BRL, Grand Island, N.Y.). Transduced cells were selected for 3 weeks in RPMI 1640 medium containing 10% fetal bovine serum and 1 mg of G418 (Geneticin; GIBCO BRL) per ml. The clones expressing the highest levels of Bcl-2 and Bcl-X_L were used for this study. Lysates were evaluated for Bcl-2 and Bcl-X_L expression by immunoblot analysis.

For transient transfection, Lipofectin reagent was used to transfect cDNA plasmids by following the protocol provided by the manufacturer (GIBCO BRL). After transfection, the cells were incubated with complete medium for one additional day. These cells were then used for experiments.

Calcium measurements. For the measurement of intracellular Ca^{2+} concentration by flow cytometry, 10^7 cells were loaded for 45 min at 37°C with 5 μM indo-1/AM. The cells were washed, resuspended at 10^6/ml in HBSS containing 1.4 mM $CaCl_2$, 10 mM HEPES, and 10% fetal bovine serum, and maintained at 37°C while being run on the flow cytometer. The cells were analyzed on a FACStar^{Plus} flow cytometer (Becton Dickinson) with a Krypton laser with UV optics for excitation of the indo-1. Optimal Ca^{2+}-sensitive ratios were obtained by measuring the violet (405-nm) light from calcium-bound dye and blue (485-nm) emitted light from unbound indo-1. The mean ratios were calculated over time by using MultiTime Kinetic Software (Phoenix Flow Systems).

For the measurement of intracellular free Ca^{2+} with the PTI Deltascan spectrofluorometer (SCAN-1; Photon Technology International), cells were loaded with 5 μM indo-1/AM at 37°C for 45 min in a medium comprising 0.14 M NaCl, 3 mM KCl, 1 mM $CaCl_2$, 1 mM $MgCl_2$, 10 mM D-glucose, 1.2 mM NaH_2PO_4, 4 mM $NaHCO_3$, 4 mM HEPES, and 1 mg of albumin per ml. Following loading, the cells were incubated at 2×10^6 cells per ml in the cuvette of a PTI Deltascan spectrofluorometer in the medium described above but with 20 mM sodium HEPES and no HCO_3^- as buffer. Fluorescence was measured at 400 nm (emission maximum from the Ca^{2+}-bound form of indo-1) and 473 nm (an isobestic point) (54).

For the measurement of intracellular Ca^{2+} by confocal microscopic imaging, cells from each group were attached to glass slides coated with 3-aminopropyltriethoxysilane (Aldrich, St. Louis, Mo.) and loaded with 5 μM indo-1/AM for 45 min at 37°C. The cells were washed for at least 45 min with Hanks balanced salt solution containing 1.4 mM $CaCl_2$, 10 mM HEPES, and 10% fetal bovine serum and visualized under a microscope in the presence or absence of TG. Calcium was imaged in fields of 75 to 100 cells by using a Zeiss LSM 410 inverted confocal microscope with 351-nm excitation from a UV Ar laser with a 40×/1.2 NA *c*-APO water immersion lens. Epifluorescence was measured at 400 to 435 nm and 473 to 497 nm on matched photomultipliers, and the ratio of these channels was used to estimate the intracellular Ca^{2+} concentration from an in vitro Ca^{2+} calibration curve.

For comparison of whole-cell and mitochondrial Ca^{2+} responses, cells were dually loaded with indo-1/AM (which distributes throughout the cell) and the mitochondrion-localizing Ca^{2+} indicator rhod-2. The cells were incubated with 5 μM rhod-2 for 30 min at 25°C, washed in Hanks balanced salt solution (containing 1.4 mM Ca^{2+} and 10% fetal bovine serum) for 45 min, and then incubated with indo-1/AM as described above. Cells dually loaded with rhod-2 and indo-1/AM remained in indicator-free medium for at least 3 h before being imaged. This method results in selective mitochondrial loading with rhod-2 (i.e., without significant extramitochondrial loading). This was confirmed in a parallel group of cells by colocalization of rhod-2 fluorescence with that of the mitochondrion-specific probe Mito Tracker Green FM (250 nM for 30 min at 25°C) and by >95% loss of rhod-2 fluorescence within 5 min after addition of 1 μM FCCP to the bath (with no significant change in indo-1/AM fluorescence). Rhod-2 fluorescence was obtained in cells coloaded with indo-1/AM by excitation at 543 nm from a He-Ne laser, measuring the emitted fluorescence with a long-pass 570 nm filter. Rhod-2 fluorescence signals were not calibrated and represent a qualitative measure of changes in mitochondrial Ca^{2+}. There was no detectable fluorescence cross talk between the rhod-2 and indo-1/AM channels. Every cell within the microscopic field was included in the assessment of Ca^{2+}. Image processing was performed with MetaMorph (Universal Imaging Corp., West Chester, Pa.) on a Pentium computer.

Measurement of mitochondrial energization. Mitochondrial energization was determined as the retention of the dye 3,3′-dihexyloxacarbocyanine ($DiOC_6$)(3). Cells (5×10^5 in 500 μl of complete RPMI 1640 medium) were loaded with 100 nM $DiOC_6(3)$ during the last 30 min of treatment. The cells were then pelleted at 700 × *g* for 10 min. The supernatant was removed, and the pellet was resuspended and washed in phosphate-buffered saline (PBS) twice. The pellet was then lysed by the addition of 600 μl of deionized water followed by homo-

genization. The concentration of retained $DiOC_6(3)$ was determined on a fluorescence spectrometer (Cyto Fluor; PerSeptive Biosystems, Framingham, Mass.) at 480-nm excitation and 510-nm emission (49).

Subcellular fractionation. Mitochondrial and cytosolic (S100) fractions were prepared by resuspending cells in 0.8 ml of ice-cold buffer A (250 mM sucrose, 20 mM HEPES, 10 mM KCl, 1.5 mM $MgCl_2$, 1 mM EDTA, 1 mM EGTA, 1 mM dithiothreitol [DTT], 17 μg of phenylmethylsulfonyl fluoride per ml, 8 μg of aprotinin per ml, 2 μg of leupeptin per ml [pH 7.4]) (20). The cells were passed through an ice-cold cylinder cell homogenizer. Unlysed cells and nuclei were pelleted by a 10-min centrifugation at 750 × *g*. The supernatant was centrifuged at 10,000 × *g* for 25 min. This pellet was resuspended in buffer A and represents the mitochondrial fraction. The supernatant was centrifuged at 100,000 × *g* for 1 h. The supernatant from this final centrifugation represents the S100 fraction.

Lysate preparation. For determination of JNK activity, cells were collected by centrifugation at 300 × *g* for 5 min at 4°C. The cell pellets were washed with cold PBS and solubilized with ice-cold JNK lysis buffer (25 mM HEPES [pH 7.5], 300 mM NaCl, 1.5 mM $MgCl_2$, 0.2 mM EDTA, 0.1% Triton X-100, 20 mM β-glycerophosphate, 0.1 mM sodium orthovanadate, 0.5 mM DTT, 100 μg of phenylmethylsulfonyl fluoride per ml, 2 μg of leupeptin per ml). The cellular extract was then centrifuged for 30 min at 1,200 × *g* to remove debris. The supernatant was used immediately or aliquoted and stored at −70°C for future use.

For Western blotting, cells were lysed in a buffer containing 10 mM Tris-HCl (pH 7.6), 150 mM NaCl, 0.5 mM EDTA, 1 mM EGTA, 1% sodium dodecyl sulfate (SDS), 1 mM sodium orthovanadate, and a mixture of protease inhibitors (1 mM phenylmethylsulfonyl fluoride, 1 μg of pepstatin A per ml, 2 μg of aprotinin per ml). The lysates were then sonicated for 10 s and centrifuged for 20 min at 1,200 × *g*. The supernatants were used to perform SDS-polyacrylamide gel electrophoresis (PAGE) or stored at −70°C.

Measurement of JNK activity. JNK1 was immunoprecipitated and kinase activity was measured by using an immunokinase complex assay with GST–c-Jun as a substrate as described previously (30). Briefly, cell lysates (200 μg of protein) were first incubated overnight at 4°C with 10 μg of polyclonal anti-JNK1 and then incubated with 20 μl of Sepharose A-conjugated protein A for an additional 1 h. The beads were pelleted and washed three times with cold PBS containing 1% Nonidet P-40 and 2 mM sodium orthovanadate, once with cold 100 mM Tris-HCl (pH 7.5) buffer containing 0.5 M LiCl, and once with cold kinase reaction buffer (12.5 mM morpholinepropanesulfonic acid [MOPS] [pH 7.5], 12.5 mM β-glycerophosphate, 7.5 mM $MgCl_2$, 0.5 mM EGTA, 0.5 mM NaF, 0.5 mM sodium orthovanadate). The kinase reaction was performed in the presence of 1 μCi of [γ-^{32}P]ATP, 20 μM ATP, 3.3 μM DTT, and 3 μg of substrate GST–c-Jun-(1–135) in kinase reaction buffer for 30 min at 30°C and stopped by addition of 10 μl of 5× Laemmli loading buffer. The samples were heated for 5 min at 95°C and analyzed by SDS-PAGE (12% polyacrylamide). Phosphorylated substrate c-Jun was visualized by autoradiography. The optical density of autoradiograms was determined with the NIH Image program. The kinase activity was expressed as fold of control.

Measurement of nitric oxide. For the measurement of nitric oxide (NO), the Griess reagent kit (Molecular Probes, Inc.) was used. This assay involves the use of the Griess diazotization reaction to spectrophotometrically detect nitrite formed by the spontaneous oxidation of NO under physiological conditions. The detection limit for this method is between 0.1 and 1.0 μM nitrite. Nitrite concentrations were measured in cell lysates.

Western blot analysis. Equal amounts of lysate protein (40 μg/lane) were subjected to SDS-PAGE with either 10% or 8 to 16% polyacrylamide gels and electrophoretically transferred to nitrocellulose. Nitrocellulose blots were first blocked with 10% nonfat dry milk in TBST buffer (20 mM Tris-HCl [pH 7.4], 500 mM NaCl, 0.01% Tween 20) and then incubated overnight at 4°C with primary antibody in TBST containing 5% bovine serum albumin. Immunoreactivity was detected by sequential incubation of horseradish peroxidase-conjugated secondary antibody, and specific complexes were detected by the enhanced chemiluminescence technique.

Measurement of caspase-3 activity. ApoAlert caspase assay kit (Clontech Laboratories, Inc., Palo Alto, Calif.) was used to measure caspase-3 activity. The ApoAlert caspase-3 fluorescence assay kit detects the shift in fluorescence emission of 7-amino-4-trifluoromethyl coumarin (AFC). AFC is conjugated to a specific tetrapeptide sequence (DEVD-AFC). Normally the conjugate emits blue light. Upon cleavage of the substrate by protease, the liberated AFC emits a yellow-green fluorescence at 505 nm. Assays were performed directly on crude cell lysates as specified by the manufacturer.

Apoptosis. For detection of apoptotic cells, the cells were first washed twice with cold PBS and then fixed with 4% paraformaldehyde for 30 min. The fixed cells were washed again with PBS and stained with 1 μg of DAPI per ml for 30 min. The apoptotic cells were examined under a fluorescence microscope. Cells containing condensed or fragmented nuclei were scored as apoptotic. Data are expressed as a percentage of apoptotic cells in total counted cells.

For detection of apoptosis by annexin V fluorescence and propidium iodide staining, a kit was purchased from R & D Systems. We used the procedure as described by the manufacturer.

Nucleosome ELISA. The nucleosome ELISA allows the quantitation of apoptotic cells in vitro by DNA affinity-mediated capture of free nucleosomes followed by their anti-histone-facilitated detection. In this assay, mono- and oligonucleosomes are captured on precoated DNA-binding proteins. Standards were provided in the kit to measure number of nucleosomes per milliliter. Based on the standard curve, we measured nucleosomes (units per milliliter) in the cell lysates. Cells (2×10^6) were seeded into 24-well plates for 36 h in the presence or absence of various drugs (see the figure legends). They were harvested for the nucleosome ELISA as specified by the manufacturer (Oncogene Research Products, Cambridge, Mass.). Anti-histone 3 biotin-labeled antibody binds to the histone component of captured nucleosomes and is detected following incubation with streptavidin-linked horseradish peroxidase (SA-HRP) conjugate. HRP catalyzes the conversion of colorless tetramethylbenzidine to blue. The addition of stop solution changes the color to yellow, the intensity of which is proportional to the number of nucleosomes in the sample.

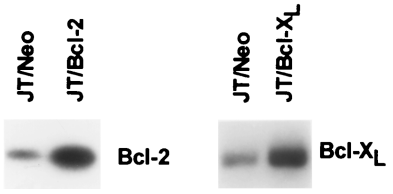

FIG. 1. Increased levels of Bcl-2 and Bcl-X_L in JT/Bcl-2 and JT/Bcl-X_L cells, respectively. Western blots show the increased expression of Bcl-2 or Bcl-X_L in Jurkat T cells transfected with exogenous full-length human Bcl-2 or Bcl-X_L.

RESULTS

Overexpression of Bcl-2 or Bcl-X_L does not alter TG-induced calcium release. Jurkat T lymphocytes were transfected with human Bcl-2 (JT/Bcl-2) or Bcl-X_L (JT/Bcl-X_L) to measure the effects of these antiapoptotic genes on TG-induced cytoplasmic calcium accumulation. Transfection of Bcl-2 and Bcl-X_L genes in Jurkat T cells resulted in significant overexpression of these proteins (Fig. 1). Treatment of JT/Neo cells with TG resulted in a transient increase in the intracellular free calcium level that varied in a dose-dependent manner (1 to 100 nM) (data not shown). Overexpression of Bcl-2 or Bcl-X_L in Jurkat T cells had no significant effect on the transient increase in the intracellular free calcium level induced by 50 nM TG compared to overexpression of Neo (Fig. 2A). Pretreatment of Jurkat cells with BAPTA-AM abrogated the transient increase in intracellular free calcium levels due to TG treatment (data not shown). We further examined the involvement of extracellular calcium in TG-induced transient calcium release by using EGTA (an extracellular calcium chelator), which was added at 2 mM to remove any contribution of extracellular calcium to the 400-nm emission (Fig. 2B). TG (500 nM) gave a large and transient increase in the 400-nm/473-nm ratio and hence in cytosolic free Ca^{2+}, reflecting the release of ER Ca^{2+} into the cytosol (Fig. 2B). Ionomycin (5 μM) addition released Ca^{2+} from other cellular compartments. Subsequent addition of 8 mM EGTA and 12 mM $CaCl_2$ gave fluorescence emission ratio minimum (R_{min}) and maximum (R_{max}) values, respectively (Fig. 2B). We next sought to compare the FCCP- (a mitochondrial uncoupler) and TG-releasable Ca^{2+} stores (Fig. 2C). Addition of the uncoupling agent FCCP (0.25 μM) allowed the mobilization and visualization of the mitochondrial Ca^{2+} pool (Fig. 2C). Subsequently added TG (500 nM) gave a large and transient increase in the cytosolic free Ca^{2+} concentration (Fig. 2C). These data suggest that intracellular free-Ca^{2+} store release induced by TG was not affected by extracellular Ca^{2+} influx.

Since Bcl-2 and Bcl-X_L did not block TG-induced transient intracellular free Ca^{2+} levels in cells, we sought to determine the calcium levels in the mitochondria and cytosol at 3 h (Fig. 3). At 3 h, overexpression of Bcl-2 or Bcl-X_L had no effect on the level of mitochondrial or cytosolic free calcium, which was similarly increased by TG in all cell lines (Fig. 3A and B). However, at 36 h, cells overexpressing Bcl-2 or Bcl-X_L had

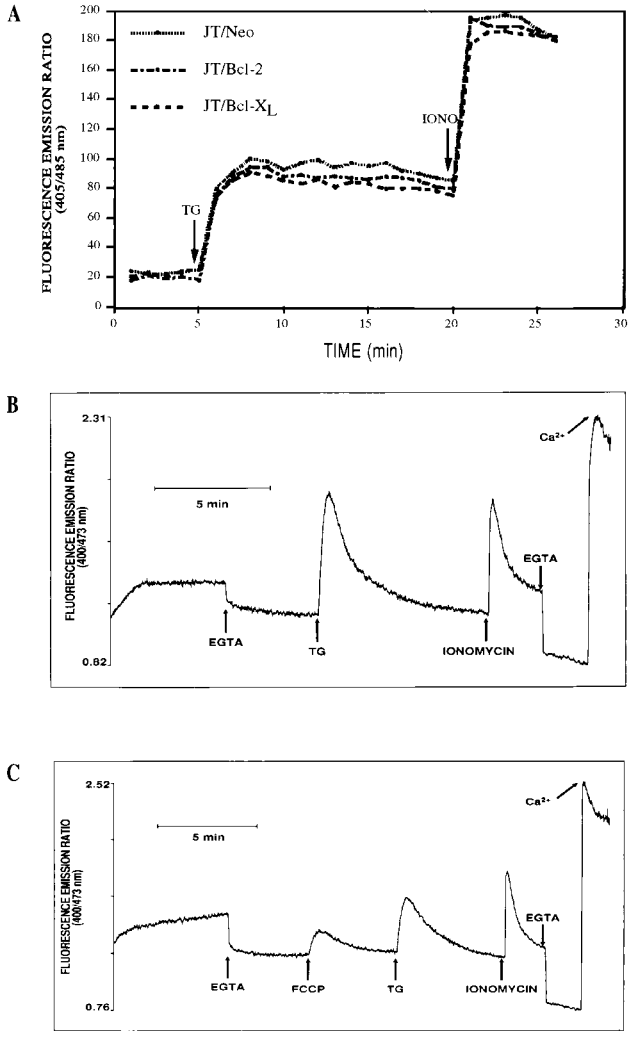

FIG. 2. Transient intracellular calcium release by TG, FCCP, and ionomycin. (A) JT/Neo, JT/Bcl-2, and JT/Bcl-X_L cells were loaded for 45 min at 37°C with 3 μM indo-1/AM and then treated with TG (50 nM) and ionomycin (5 μM). The cells were analyzed on a FACStar^{Plus} flow cytometer (Becton Dickinson) with a Krypton laser with UV optics for excitation of the Indo-1/AM. Optimal Ca^{2+} sensitivity ratios were obtained by measuring the violet (405-nm) light from calcium-bound dye and blue (485-nm) emitted light from unbound Indo-1/AM. (B) Intracellular free Ca^{2+} in Jurkat cells was measured with a PTI Deltascan spectrofluorometer. EGTA (2 mM) was added to remove any contribution of extracellular calcium to the 400-nm emission. TG (500 nM) gave a large and transient increase in 400-nm/473-nm ratio, and hence cytosolic free Ca^{2+}, reflecting the release of ER Ca^{2+} into the cytosol. Addition of 5 μM ionomycin released Ca^{2+} from other cellular compartments. Subsequent addition of 8 mM EGTA and 12 mM $CaCl_2$ gave R_{min} and R_{max}, respectively. (C) Intracellular free Ca^{2+} in Jurkat cells was measured with a PTI Deltascan spectrofluorometer. Addition of the mitochondrial uncoupling agent FCCP (0.25 μM) allowed the mobilization and visualization of the mitochondrial Ca^{2+} pool. The remainder of the experiment was done by the method described for panel B.

significantly lower levels of intracellular free calcium (Fig. 4A). Further, TG-induced apoptosis was correlated with intracellular calcium levels in excess of 600 nM, which were correspondingly reduced in JT/Bcl-2 and JT/Bcl-X_L cells (Fig. 4B). The elevated Ca^{2+} levels at 36 h occur at a time when the apoptosis process is ongoing in cells not overexpressing Bcl-2 and Bcl-X_L. Thus, the late alterations in Ca^{2+} levels are a consequence of apoptosis. Early calcium fluxes are not influenced by Bcl-2 and Bcl-X_L expression.

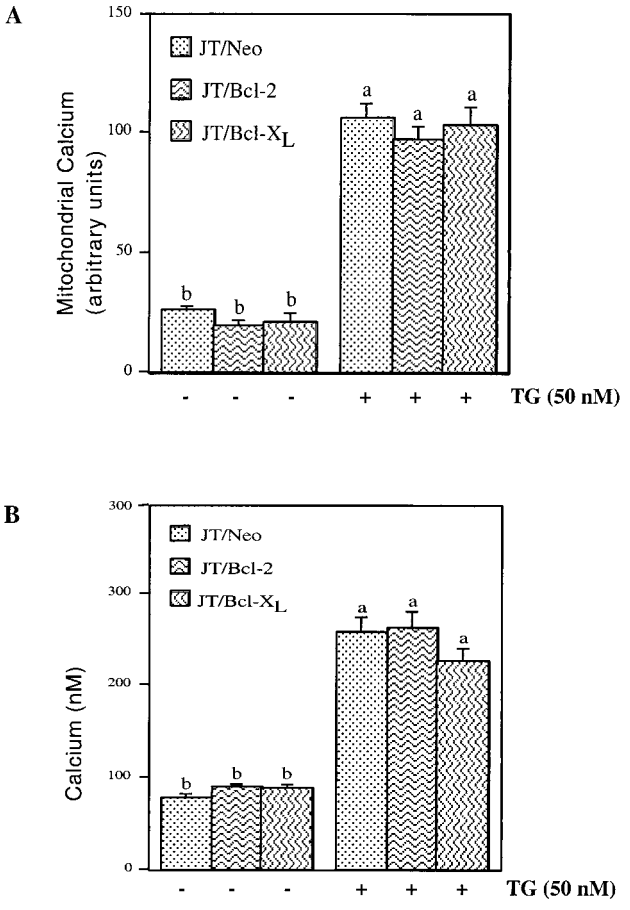

FIG. 3. Overexpression of Bcl-2 or Bcl-X_L has no effect on TG-induced changes in mitochondrial and cytosolic free-calcium levels at 3 h. JT/Neo, JT/Bcl-2, and JT/Bcl-X_L cells were treated with TG (50 nM) for 3 h, loaded with indo-1/AM and rhod-2, and analyzed for mitochondrial (A) and cytosolic free (B) calcium levels by confocal imaging microscopy (see Materials and Methods for details). The data are the means and standard errors. Significant differences ($P < 0.05$) among groups were determined by analysis of variance with multiple comparisons by the Student-Neuman Keul test and are indicated by different letters. Histograms denoted by a common letter are not significantly different in group comparisons. Means among groups denoted by dissimilar letters are statistically significant.

A rise in the intracellular calcium level is necessary for TG-induced apoptosis. We first determined the effects of Bcl-2 and Bcl-X_L on TG-induced apoptosis (as measured by nucleosome ELISA) over time (Fig. 5A). Treatment of JT/Neo cells with TG (50 nM) resulted in induction of apoptosis which began after 6 h and increased over a period of 48 h (Fig. 5A). Overexpression of Bcl-2 or Bcl-X_L inhibited TG-induced apoptosis over a period of 48 h (Fig. 5A). To evaluate the relationship between intracellular calcium levels and apoptosis, we used irreversible (TG) and reversible (CPA) inhibitors of the ER calcium-ATPase pump. These compounds are known to increase intracellular calcium levels. Treatment of wild-type Jurkat cells with TG or CPA resulted in the induction of apoptosis in a dose-dependent manner at 36 h (Fig. 5B and C). We next examined the source of the calcium that accumulated after TG or CPA treatment. BAPTA-AM was used to chelate cytoplasmic calcium, and EGTA was used to chelate extracellular calcium. Cells were pretreated with BAPTA-AM (10 μM) for 45 min, washed with PBS, and reseeded in culture medium with or without TG or CPA. BAPTA-AM abolished the apop-

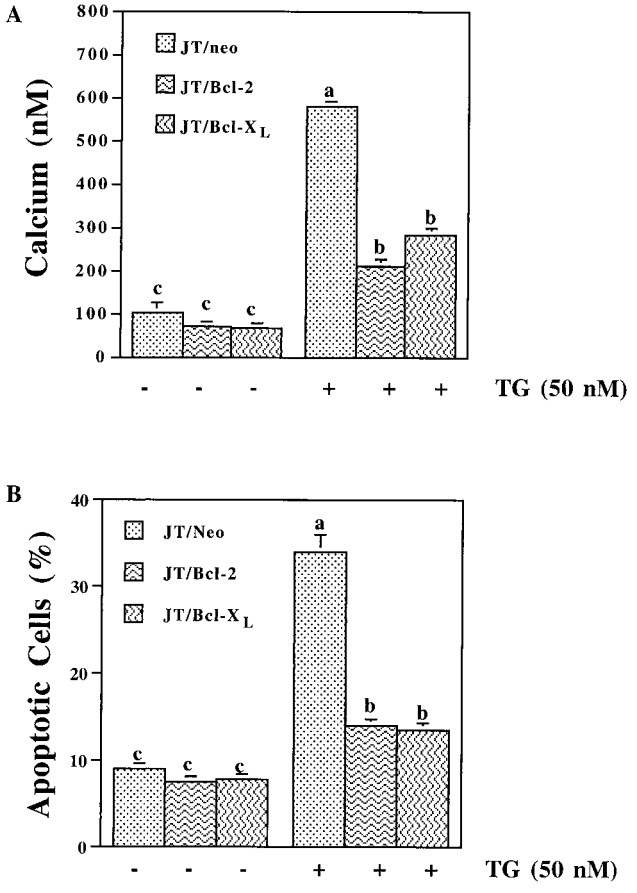

FIG. 4. Overexpression of Bcl-2 or Bcl-X_L prevents TG-induced intracellular free Ca^{2+} accumulation and apoptosis at 36 h. (A) JT/Neo, JT/Bcl-2, and JT/Bcl-X_L cells were treated with 50 nM TG for 36 h, loaded with indo-1/AM, and analyzed for intracellular free Ca^{2+} levels by confocal imaging microscopy. (B) JT/Neo, JT/Bcl-2, and JT/Bcl-X_L cells were treated with TG for 36 h and stained with annexin V-fluorescein isothiocyanate and propidium iodide to examine apoptotic cells. The data are the means and standard errors. Significant differences ($P < 0.05$) among groups were determined by analysis of variance with multiple comparisons by the Student-Neuman Keul test and are indicated by different letters. Histograms denoted by a common letter are not significantly different in group comparisons. Means among groups denoted by dissimilar letters are statistically significant.

totic effects of TG or CPA (Fig. 5B and C). By contrast, the chelation of extracellular calcium with 2 mM EGTA had no significant effect on TG- or CPA-induced apoptosis (data not shown). These data suggest that intracellular free calcium accumulation plays a critical initiating role in TG- or CPA-induced apoptosis.

Because TG and CPA induced apoptosis in Jurkat cells, we next examined the effects of Bcl-2 and Bcl-X_L overexpression on TG- or CPA-induced apoptosis (Fig. 5D and E). Treatment of Jurkat cells with TG or CPA resulted in the induction of apoptosis in a dose-dependent manner at 36 h. Overexpression of Bcl-2 or Bcl-X_L blocks TG- or CPA-induced apoptosis (Fig. 5D and E) in Jurkat cells. Because Ca^{2+} release is similar in wild-type and Bcl-2- and Bcl-X_L-overexpressing cells, Bcl-2 and Bcl-X_L must be blocking apoptosis at a point in the pathway downstream of Ca^{2+} release.

Bcl-2 or Bcl-X_L prevents the release of cytochrome *c*. Mitochondria appear to play an important role in the early events of apoptosis (4). Both mitochondrial depolarization and the loss of cytochrome *c* from the mitochondrial intermembrane space have been proposed as early central events in apoptotic cell death (52, 70). Whether cytochrome *c* release occurs before the loss of mitochondrial membrane potential or as a result of the loss of inner membrane potential remains controversial (29, 59, 70). Since the cell survival proteins Bcl-2 and Bcl-X_L localize to the outer mitochondrial membrane, the effects of Bcl-2 or Bcl-X_L overexpression on cytochrome *c* redistribution and mitochondrial membrane depolarization in response to TG were investigated.

We next determined the presence of cytochrome *c* in the cytosolic and mitochondrial fractions of cells treated with TG. The subcellular localization of cytochrome *c*, which normally resides in the mitochondrial intermembrane space, was first assessed at various times following TG treatment (Fig. 6A). Treatment of wild-type or JT/Neo Jurkat cells with TG resulted in the release of cytochrome *c* from the mitochondria in a time-dependent manner (Fig. 6A). In Jurkat cells, the release of cytochrome *c* began at 2 h and reached a plateau at 4 h (Fig. 6A). At 4 h after 100 nM TG treatment, Jurkat cells had not yet undergone apoptosis as measured by DAPI staining (data not shown). We next examined the effects of Bcl-2 and Bcl-X_L on the cytochrome *c* release after 4 h of 100 nM TG treatment (Fig. 6B). There was no cytochrome *c* in the cytosol of untreated JT/Neo, JT/Bcl-2, or JT/Bcl-X_L cells (Fig. 6B). When cells were treated with TG (100 nM) for 4 h, cytochrome *c* was detected in the cytosol of JT/Neo cells (Fig. 6B). By contrast, cytochrome *c* was not detected in the cytosol of TG-treated JT/Bcl-2 or JT/Bcl-X_L cells (Fig. 6B). The caspase inhibitor z-VAD-fmk did not block TG-induced cytochrome *c* release from mitochondria (Fig. 6B). JT/Bcl-2 and JT/Bcl-X_L cells were >92 to 95% viable after 4 h of TG treatment (data not shown). In contrast to the cytochrome *c* release, the inner mitochondrial membrane protein cytochrome oxidase remained in the mitochondrial fraction in all cell groups under all conditions tested (Fig. 6B). Thus, Bcl-2 and Bcl-X_L appear to act upstream of mitochondrial cytochrome *c* release from mitochondria in the prevention of TG-induced apoptosis.

The activation of caspases appears to be essential for the implementation of apoptosis (62). Bcl-2 and Bcl-X_L have recently been proposed to regulate caspase activation (8). Recent data have shown that cytochrome *c* is involved in the activation of caspase(s) (63). Treatment of JT/Neo cells with 100 nM TG resulted in an increase in caspase-3 activity (Fig. 6C). Bcl-2 or Bcl-X_L overexpression blocked caspase-3 activation (Fig. 6C). To assess the involvement of caspase(s) in TG- or CPA-induced apoptosis, we used the caspase inhibitors z-VAD-fmk and z-DEVD-fmk. As shown above, TG or CPA induced apoptosis in Jurkat cells in a dose-dependent manner (Fig. 5D and E). In addition, Z-VAD-fmk and z-DEVD-fmk blocked TG- and CPA-induced apoptosis in Jurkat cells (Fig. 6D). These data are consistent with the hypothesis that the inhibition of cytochrome *c* release in Bcl-2- and Bcl-X_L-overexpressing cells results in a failure to activate caspase-3.

TG causes mitochondrial depolarization that is inhibited by Bcl-2 or Bcl-X_L but not by z-DEVD-fmk. Mitochondrial permeability transition (MPT) refers to the regulated opening of a large, nonspecific pore in the inner mitochondrial membrane (4). The MPT causes the loss of the mitochondrial membrane potential ($\Delta\Psi_m$) (44). The fluorescent dye $DiOC_6(3)$ localizes to mitochondria, and the MPT reduces the accumulation of $DiOC_6(3)$ as a consequence of the loss of $\Delta\Psi_m$ (66). Treatment of JT/Neo cells with TG produced a steady decline in $\Delta\Psi_m$ (Fig. 7A). Within 4 h, more than 30% of the dye was lost from the cells (Fig. 7A). The time-dependent loss of $DiOC_6(3)$ fluorescence in Jurkat cells due to TG treatment was pre-

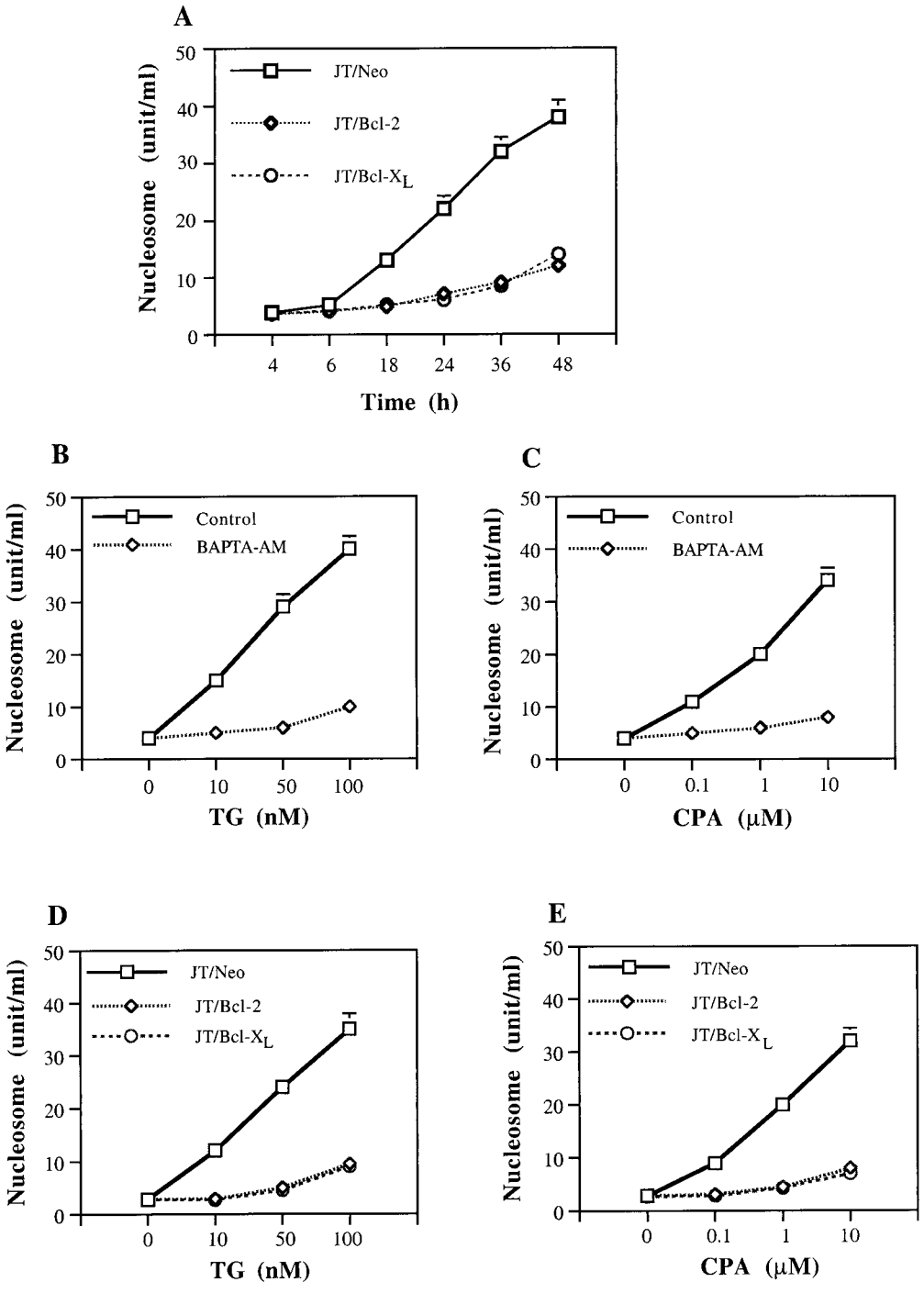

FIG. 5. Inhibition of TG- or CPA-induced apoptosis by chelating intracellular calcium or overexpressing Bcl-2 and Bcl-X_L. (A) Time course of TG-induced apoptosis in JT/Neo, JT/Bcl-2, and JT/Bcl-X_L cells. Cells were treated with TG (50 nM) for 4, 6, 18, 24, 36, and 48 h. (B and C) Chelation of intracellular calcium by BAPTA-AM blocks TG- or CPA-induced apoptosis. Cells were pretreated with BAPTA-AM (10 μM) for 45 min, washed, reseeded and treated with TG (10, 50, or 100 nM), or CPA (0.1, 1, or 10 μM) for 36 h. (D and E) Overexpression of Bcl-2 or Bcl-X_L blocks TG- or CPA-induced apoptosis. Cells were treated with TG (10, 50, or 100 nM) or CPA (0.1, 1, or 10 μM) for 36 h. A nucleosome ELISA was used to measure apoptosis.

vented by the overexpression of Bcl-2 or Bcl-X_L (Fig. 7A). Consistent with its inability to prevent the loss of cytochrome *c* release (Fig. 6B), the caspase inhibitor z-DEVD-fmk had no effect on TG-induced mitochondrial depolarization (14) (Fig. 7B). These data suggest that Bcl-2 and Bcl-X_L regulate the release of mitochondrial factors that are required for caspase activation, and the caspases act downstream of mitochondrial apoptotic events since the caspase inhibitors have no effect on cytochrome *c* release and loss of $\Delta\Psi_m$ caused by TG.

TG activates the JNK/SAPK pathway. Activation of the JNK pathway has been implicated in initiating apoptosis in response to several stimuli (6, 7, 11, 12, 30, 35, 67). To test the hypoth-

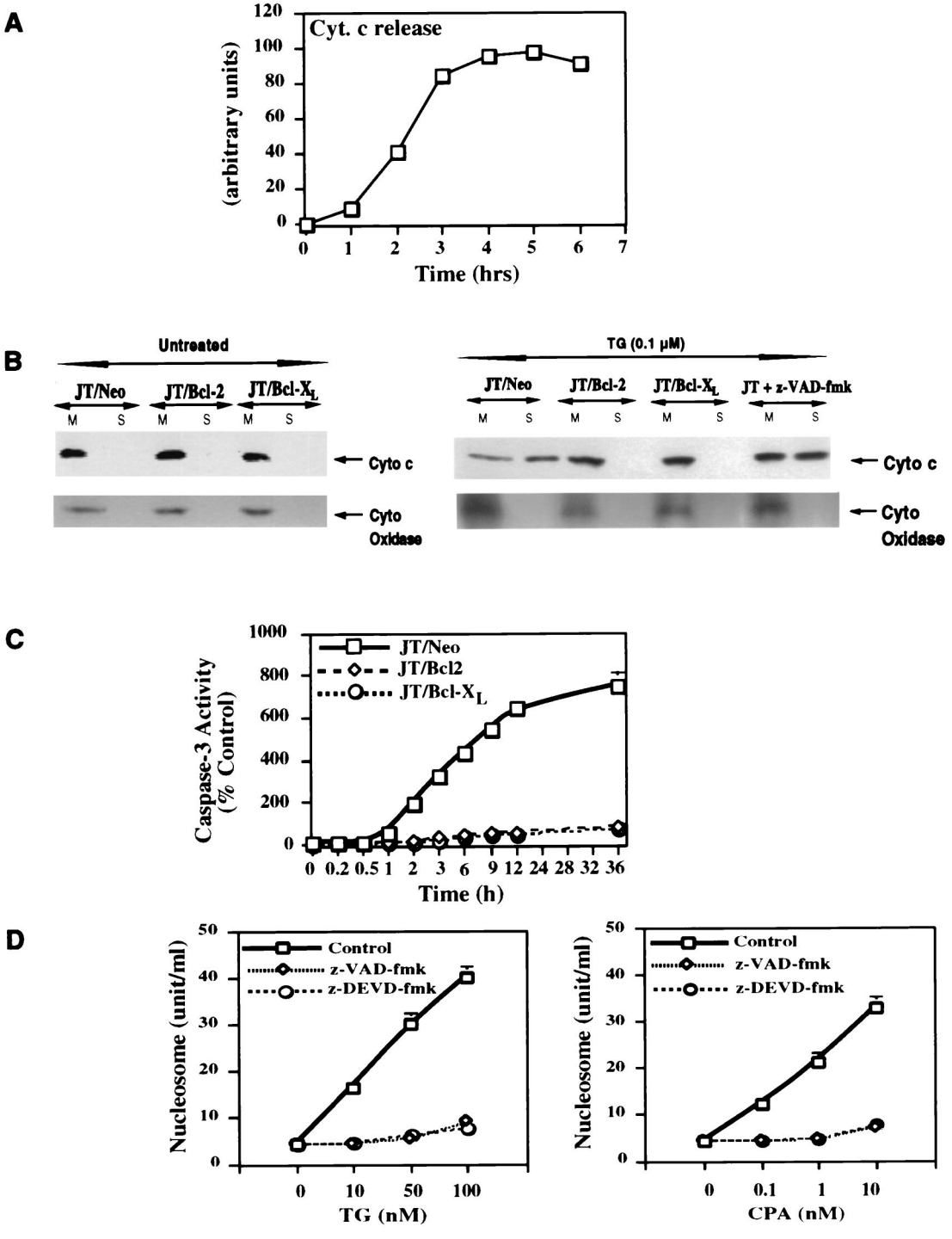

FIG. 6. Bcl-2 and Bcl-X_L prevent the redistribution of cytochrome *c* in cells undergoing apoptosis. (A) Time course of cytochrome *c* release in Jurkat cells treated with TG. The release of cytochrome *c* in the cytosolic extract was determined by Western blot analysis and was quantified by densitometric scanning of the autoradiograph and plotted against time in hours after TG treatment. (B) Redistribution of cytochrome *c* in Bcl-2- and Bcl-X_L-overexpressing Jurkat cells. JT/Neo, JT/Bcl-2, and JT/Bcl-X_L cells were treated with 100 nM TG. Jurkat T cells were pretreated with the caspase inhibitor z-VAD-fmk (50 μM) for 1 h prior to addition of TG (right panel). After 3 h, the cells were mechanically lysed and separated into mitochondrial (M) and S100 (S) fractions. The amounts of cytochrome *c* and cytochrome oxidase (subunit IV) present in each fraction were determined by Western blot analysis. (C) Bcl-2 or Bcl-X_L blocks TG-induced caspase-3 activation. Jurkat cells were treated with TG (100 nM) for various times. Caspase-3 activity was measured as specified by the manufacturer (see Materials and Methods). (D) The caspase inhibitors z-VAD-fmk and z-DEVD-fmk block TG- and CPA-induced apoptosis. Jurkat T cells were pretreated with the caspase inhibitor z-VAD-fmk (50 μM) or z-DEVD-fmk (50 μM) for 1 h and then treated with TG or CPA for an additional 36 h. Apoptosis was measured by a nucleosome ELISA.

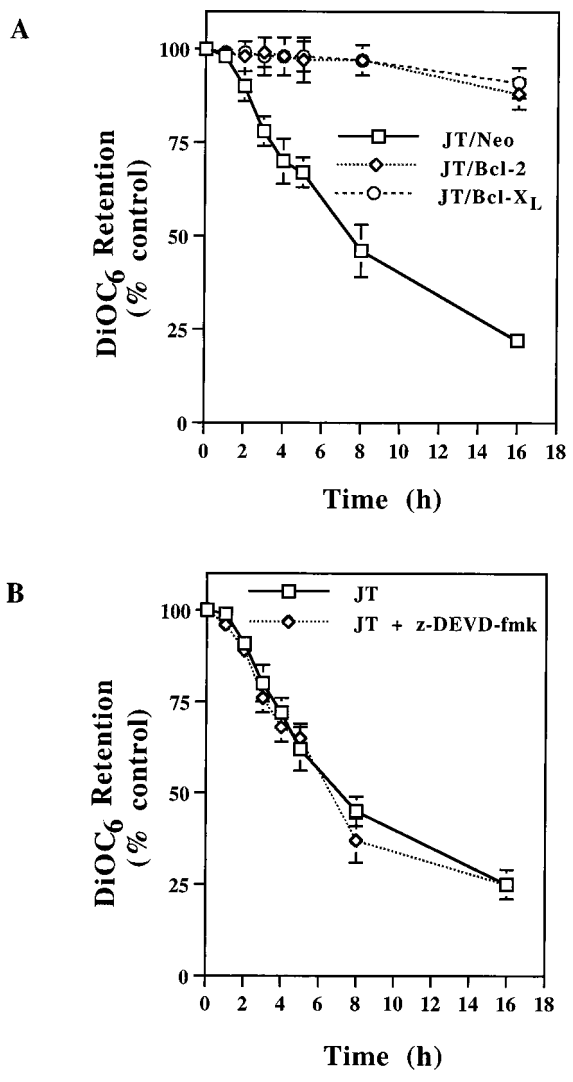

FIG. 7. TG causes mitochondrial depolarization that is inhibited by Bcl-2 or Bcl-X_L but not by the caspase inhibitor z-DEVD-fmk. (A) JT/Neo, JT/Bcl-2, and JT/Bcl-X_L cells were treated with TG (100 nM) for various times or left untreated. During the last 30 min of treatment, $DiOC_6(3)$ was added. An aliquot of the cells was used for the determination of cell-associated $DiOC_6(3)$ fluorescence. (B) Jurkat cells were pretreated for 30 min with z-DEVD-fmk before addition of 100 nM TG, and uptake of $DiOC_6(3)$ was determined at the times indicated.

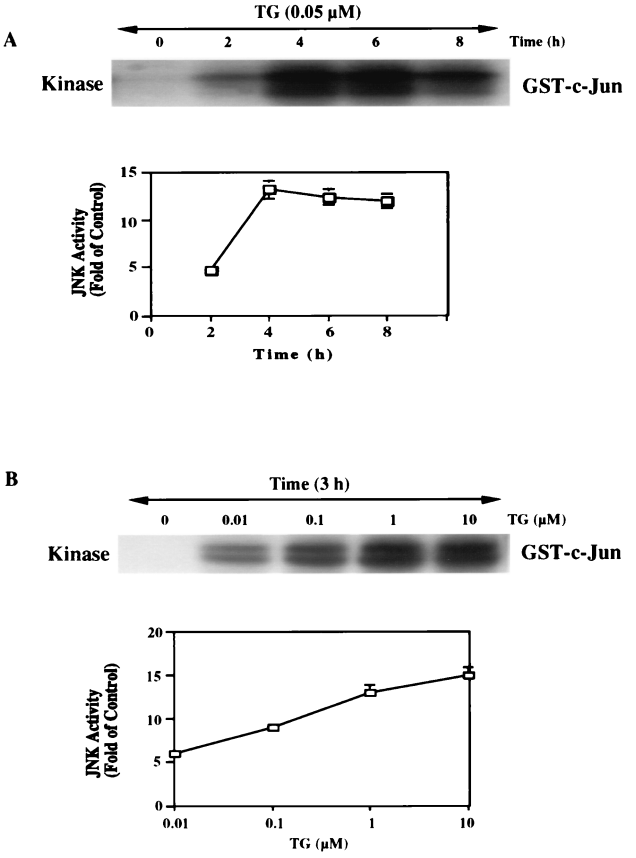

FIG. 8. TG induces JNK activation in a time- and dose-dependent manner. Jurkat T lymphocytes were treated with TG for various times. The cell lysates were prepared and immunoprecipitated with 10 μg of polyclonal anti-JNK1 antibody followed by 20 μl of Sepharose A-conjugated protein A. The kinase reaction was performed by the procedures described in Materials and Methods. (A) Time course of the kinase reaction. The top figure represents the autoradiogram of [γ-^{32}P]ATP incorporation into exogenous GST–c-Jun-(1–135). The amount of cell lysate used was 200 μg of protein in each lane. The bottom figure is a plot of JNK activity against time. The values in this figure are means and standard errors of three determinations. (B) Dose response of JNK activation. Anti-JNK1 immunocomplexes were obtained with lysates of cells treated with various doses of TG for 3 h. The JNK assay was performed as described in Materials and Methods. The top figure is a representative autoradiogram of three independent experiments. The bottom figure shows quantified data from three determinations (means and standard errors).

esis that TG-induced apoptosis may involve the JNK pathway, we examined the effects of TG, which include JNK activation and the phosphorylation of c-Jun, on this pathway.

We first characterized the JNK assay by using wild-type Jurkat cells (Fig. 8). The kinase activity increased between 0 and 4 h after TG treatment and reached a plateau thereafter (Fig. 8A). The kinase activity was also increased with the various doses of TG treatment over 3 h (Fig. 8B). Thus, TG-induced apoptosis includes JNK activation. Based on these results, we used 100 nM TG and 4-h incubation times for further experiments.

Overexpression of Bcl-2 or Bcl-X_L blocks JNK/SAPK activation by TG. We next examined the effects of TG on the activation of mitogen-activated protein (MAP) kinases (JNK, ERK, and p38) by using JNK, ERK, and p38 antibodies specific for the phosphorylated and activated forms of these kinases. Western blot analyses revealed that TG (100 nM for 4 h) activated the JNK pathway in JT/Neo cells and that the activation of JNK was blocked in JT/Bcl-2 and JT/Bcl-X_L cells (Fig. 9A). This phospho-specific antibody can recognize both phospho-JNK1 (46 kDa, a lower band) and phospho-JNK2 (54 kDa, a higher band) (Fig. 9A). The immunoblot with JNK1-specific antibody revealed that the total JNK1 protein level did not change significantly in JT/Neo, JT/Bcl-2, and JT/Bcl-X_L cells (Fig. 9A). Only modest activation of ERK was noted in response to TG (100 nM) treatment, and the level did not differ significantly in JT/Neo, JT/Bcl-2, and JT/Bcl-X_L cells (Fig. 9B). The immunoblot with ERK2-specific antibody revealed that ERK2 protein did not change in JT/Neo, JT/Bcl-2, and JT/Bcl-X_L cells (Fig. 9B). To evaluate the involvement of ERK in TG-induced apoptosis, we used a specific inhibitor of MEK1/2 (PD098059), kinases upstream of ERK1/2. Cells were pretreated with 10 μM MEK1/2 inhibitor (PD098059) for 1 h and then incubated with 100 nM TG for 36 h. The ERK inhibitor PD098059 had no effect on TG-induced apoptosis

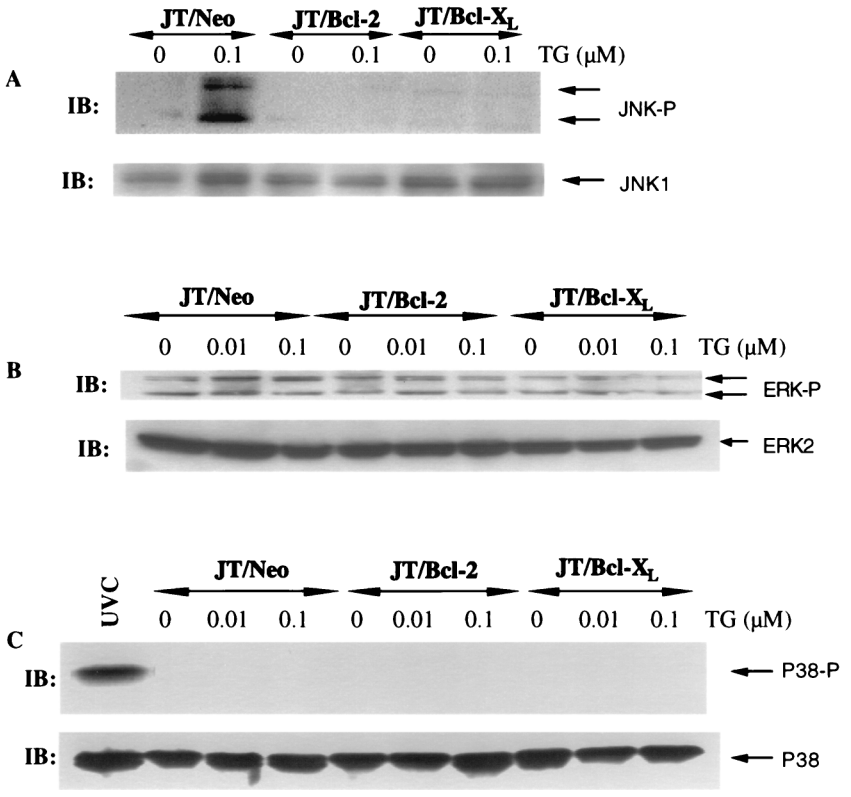

FIG. 9. Overexpression of Bcl-2 or Bcl-X_L blocks the JNK pathway. (A) JT/Neo, JT/Bcl-2, and JT/Bcl-X_L cells were treated with 100 nM TG for 4 h. The Western blots (IB) were performed with antibody specific to phosphoactive JNK (top panel) and anti-JNK1 antibody (bottom panel). (B) Cells were treated as described in panel A. The Western blots were performed with antibody specific to phosphoactive ERK (top panel) and anti-ERK2 antibody (bottom panel). (C) Cells were treated as described in panel A. The Western blots were performed with antibody specific to phosphoactive p38 (top panel) and anti-p38 antibody (bottom panel). For a positive control, a group of cells was also exposed to UVC (20 J/m^2).

(data not shown), suggesting that the modest activation of ERK is a consequence rather than the cause of TG-induced apoptosis. Interestingly, p38 was not activated in response to 100 nM TG treatment and total p38 levels did not change in JT/Neo, JT/Bcl-2, and JT/Bcl-X_L cells (Fig. 9C). In addition, p38 was activated in response to UV light (UVC) treatment. These data suggest that TG activates the JNK pathway and that TG-induced JNK activation can be blocked by Bcl-2 or Bcl-X_L overexpression.

JNK/SAPK signaling mediates TG-induced apoptosis. As mentioned previously, the JNK/SAPK pathway involves an orderly activation of proteins, MEKK1, SEK1, JNK, and c-Jun (11, 12, 25). SEK1 kinase activates JNK, and c-Jun is the substrate of JNK. We assessed the role of the JNK pathway in TG-induced apoptosis by using a dominant negative SEK1 (Lys→Arg) mutant and a c-Jun dominant negative mutant FlagΔ169.

pEBG-SEK1 (Lys→Arg) is a dominant negative kinase-inactive construct (67). In U937 cells, its transfection efficiency is about 39% (67). Expression of SEK1 (Lys→Arg) in U937 cells inhibits ceramide- or H_2O_2-induced endogenous JNK activity by 50% and completely inhibits the co-transfected hemagglutinin-tagged JNK (67). We transiently transfected this GST-tagged SEK1 dominant negative mutant into Jurkat cells. Its expression was detected by anti-GST immunoblotting (data not shown). By cotransfection with pCMV carrying the *lacZ* gene and staining with 5-bromo-4-chloro-3-indolyl-β-D-galactopyranoside (X-Gal), we calculated that the transfection efficiency was about 65 to 70% in Jurkat cells. Overexpression of this SEK-1 (Lys→Arg) mutant inhibited TG (100 nM for 4 h)-induced endogenous JNK activity by 76% compared with the control group (Fig. 10A). Accordingly, transiently transfected SEK-1 (Lys→Arg) also inhibited TG-induced phosphorylation of JNK1 as detected with the anti-phospho-JNK antibody (Fig. 10A). Furthermore, the transfection of SEK1 mutant also significantly inhibited apoptosis as measured by DAPI staining (100 nM TG for 36 h). Thus, these observations suggest that SEK1-JNK1–c-Jun activation is involved in TG-induced apoptosis.

Next, we examined the effects of a dominant negative c-Jun mutant, FLAG169, on TG-induced apoptosis. This c-Jun 169 lacks the ability to activate transcription but is still capable of dimerization and binds to DNA (18, 21). The c-Jun 169 vector is tagged by an 8-amino-acid FLAG epitope in place of NH_2-terminal 169, allowing its expression to be monitored by Western immunoblotting or immunocytochemistry with monoclonal anti-M2 (18). We transiently transfected Jurkat cells with this c-Jun 169 and detected its expression by anti-M2 immunoblotting (Fig. 10B). Its transfection efficiency was about 60 to 70% as determined by both anti-M2 immunocytochemistry and cotransfection with pCMV vector expressing *lacZ*. One day after transfection, the cells were exposed to 100 nM TG for 36 h. Compared with the situation for empty vector-transfected Jurkat cells, c-Jun 169 effectively reduced TG-induced apoptosis by more than 60% (Fig. 10B). The transfection of c-Jun 169 itself did not affect cell behavior, since no apoptosis was observed (Fig. 10B). In accordance with the above data from the negative SEK1 mutant experiments, the data with dominant

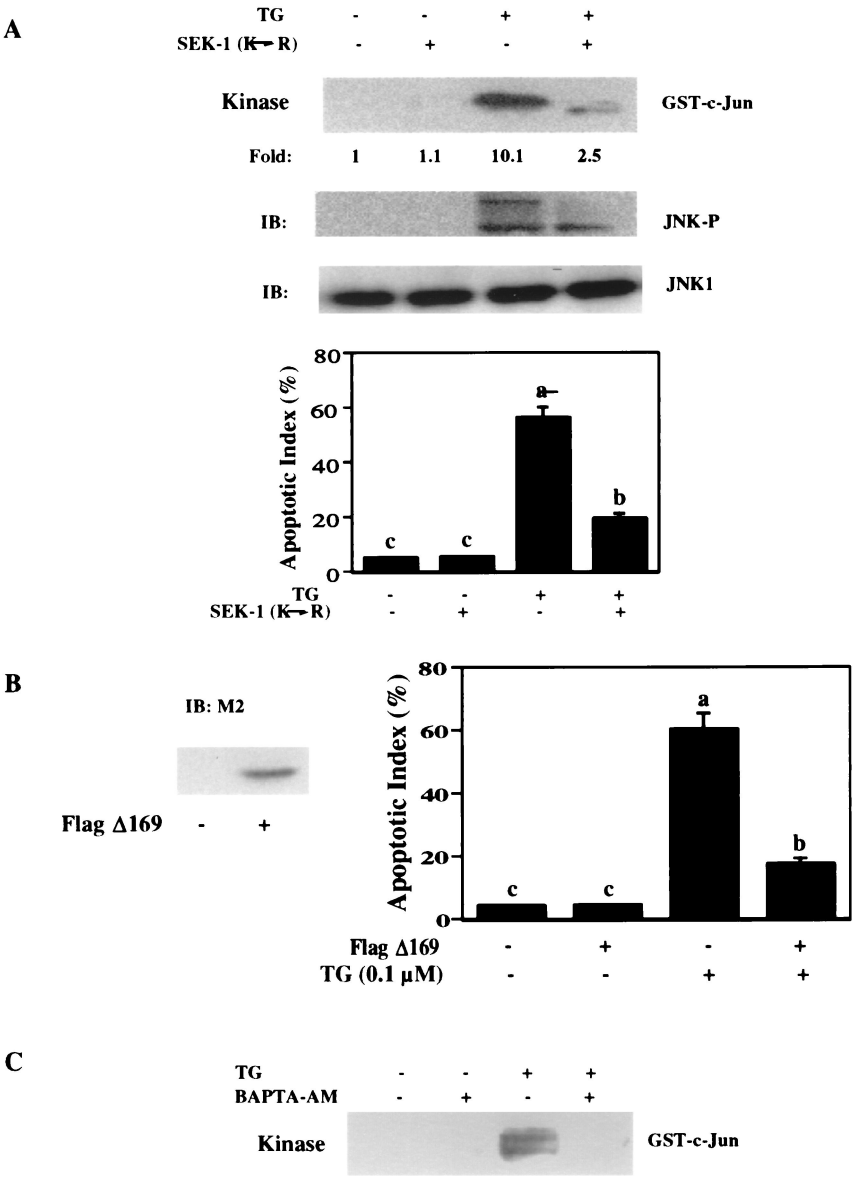

FIG. 10. Block of the JNK pathway inhibits TG-induced apoptosis. (A) A dominant negative mutant SEK1(Lys→Arg) inhibits activation of the JNK pathway and apoptosis induced by TG. Jurkat cells were plated on 60-mm dishes and transfected with a total of 2 μg of DNA of either empty vector (−) or mutated SEK1 (+) per ml. After 1 day, the cells were incubated with 100 nM TG (+) or vehicle (−) for 4 h. The cell lysates were prepared. The JNK activity and immunoblots (IB) were determined as described in the text. Antibody against phospho-specific JNK can recognize both phosphorylated JNK1 (46 kDa, lower band) and phosphorylated JNK2 (54 kDa, upper band). For apoptosis, the cells were treated with TG (100 nM) for 36 h and stained with DAPI as described in Materials and Methods. The figure shows that transfection of a dominant negative SEK1 mutant significantly inhibited JNK activation and apoptosis by TG. The data are means and standard errors. Significant differences ($P < 0.05$) among groups were determined by analysis of variance with multiple comparisons by the Student-Neuman Keul test and are indicated by different letters. Histograms denoted by a common letter are not significantly different in group comparisons. Means among groups denoted by dissimilar letters are statistically significant. (B) Dominant negative c-Jun mutant FlagΔ169 reduces TG-induced apoptosis. (Left) Immunoblotting of transfected FlagΔ169 (2 μg/ml DNA) or its empty vector (2 μg/ml) Jurkat cells with monoclonal anti-Flag (M2, 1:1,000). (Right) Percentage of apoptotic Jurkat cells due to 100 nM TG treatment for 36 h under conditions of either transfected FlagΔ169 (+, 2 μg/ml) or its empty vector (−, 2 μg/ml). The data are means and standard errors. Significant differences ($P < 0.05$) among groups were determined by analysis of variance with multiple comparisons by the Student-Neuman Keul test and are indicated by different letters. Histograms denoted by a common letter are not significantly different in group comparisons. Means among groups denoted by dissimilar letters are statistically significant. (C) Chelation of cytosolic calcium with BAPTA-AM blocks TG-induced phosphorylation and activation of JNK. Jurkat cells were pretreated with 10 μM BAPTA-AM for 45 min and then subjected to 100 nM TG treatment for 4 h. JNK activity was measured as described in Materials and Methods. The results demonstrate that chelation of cytosolic calcium with BAPTA-AM blocks TG-induced phosphorylation and activation of JNK.

negative c-Jun suggests that TG induces apoptosis through a SEK1, JNK1, and c-Jun pathway.

If the activation of JNK by TG is mediated by an increase in intracellular calcium levels, buffering of cytosolic calcium should block such an activation. Figure 5A showed that TG-induced apoptosis was blocked by the pretreatment of Jurkat cells with BAPTA-AM (10 μM). We therefore investigated whether chelation of intracellular calcium by BAPTA-AM would block TG-induced JNK activation (Fig. 10C). Treatment of Jurkat cells with 100 nM TG for 4 h resulted in the activation of JNK (Fig. 10C). When cells were pretreated with BAPTA-AM, TG did not cause JNK activation (Fig. 10C).

These results support the idea that the activation and phosphorylation of JNK by TG may be triggered by an increase in cytosolic calcium.

JNK activation occurs in response to changes in mitochondrial functions. We next evaluated whether JNK is activated before or after changes in mitochondrial functions in response to TG treatment. Transfection of a dominant negative SEK1(Lys→Arg) mutant did not block TG-induced cytochrome *c* release into the cytosol (Fig. 11A), suggesting that JNK activity is not required for cytochrome *c* release. This raises a possibility of JNK activation in response to changes in post-mitochondrial events such as caspase activation (47, 68). Pretreatment of Jurkat cells with the caspase inhibitor z-VAD-fmk or z-DEVD-fmk blocked TG-induced JNK activation (Fig. 11B). Thus, JNK activation depends upon prior caspase activation.

Although TG-induced apoptosis may involve multiple mechanisms, recent evidence suggests that generation of nitric oxide due to various stimuli may play an essential role in induction of apoptosis (1, 9, 14). Given that the TG-induced apoptosis is mediated by the JNK pathway (Fig. 10), we examined the effects of nitric oxide on TG-induced JNK activation and subsequent apoptosis. To explore the involvement of nitric oxide in TG-induced JNK activation and apoptosis, we used the NOS inhibitor L-NAME (Fig. 11C and D). The cells were first treated with L-NAME (10 mM) or D-NMMA (an arginine analogue that does not block NOS) (10 mM) or left untreated (control) for 45 min. These cells were then exposed to 100 nM TG for either 4 or 36 h to determine JNK activity and apoptotic cell death, respectively. Pretreatment of Jurkat cells with L-NAME inhibited TG-induced JNK activation and apoptosis (Fig. 11C and D). The inactive D-NMMA had no effect on TG-induced JNK activation and apoptosis (Fig. 11C and D). Thus, a NOS inhibitor protects against TG-induced apoptosis and prevents JNK activation, providing another piece of evidence for an essential role of JNK activation via NO in TG-induced apoptosis.

Bcl-2 and Bcl-X_L do not alter the nitric oxide sensitivity of Jurkat cells, but block the ability to generate nitric oxide in response to TG treatment. Since L-NAME blocked TG-induced apoptosis, we reasoned that NO was essential to the process. To assess whether Bcl-2 and Bcl-X_L were protecting the cells against NO-mediated toxicity, we exposed all these cell lines, JT/Neo, JT/Bcl-2, and JT/Bcl-X_L, to the NO donor compound SNAP, which generates NO extracellularly in the culture medium, with or without added TG. As shown in Fig. 12A, TG induces apoptosis of JT/Neo but not JT/Bcl-2 or JT/Bcl-X_L cells; however, SNAP is toxic to all three cell lines. The level of SNAP sensitivity is not greatly affected by TG. Thus, the overexpression of Bcl-2 and Bcl-X_L does not influence the ability of the cells to survive NO exposure.

There were no differences among the cell lines in NO sensitivity or in Ca^{2+} release as a consequence of TG. Therefore, we sought to examine nitric oxide production by JT/Neo, JT/Bcl-2, and JT/Bcl-X_L cells exposed to TG (Fig. 12B). Nitric oxide concentration was assessed by measuring the nitrite concentration in cells at 1, 2, and 6 h by the Griess assay. Treatment of cells with TG resulted in nitrite production as early as 1 h, and the level of nitrite increased over a period of 6 h (Fig. 12B). As expected, L-NAME (10 mM) and BAPTA-AM (10 μM) blocked TG-induced nitrite production in JT/Neo, JT/Bcl-2, and JT/Bcl-X_L cells at 1, 2, and 6 h. The overexpression of Bcl-2 or Bcl-X_L inhibited TG-induced nitrite production (Fig. 12B). The inactive inhibitor of NOS, D-NMMA, had no effect on TG-induced nitrite production. The extracellular nitric oxide donor, SNAP, increased nitrite levels 2.5- to 3-fold in

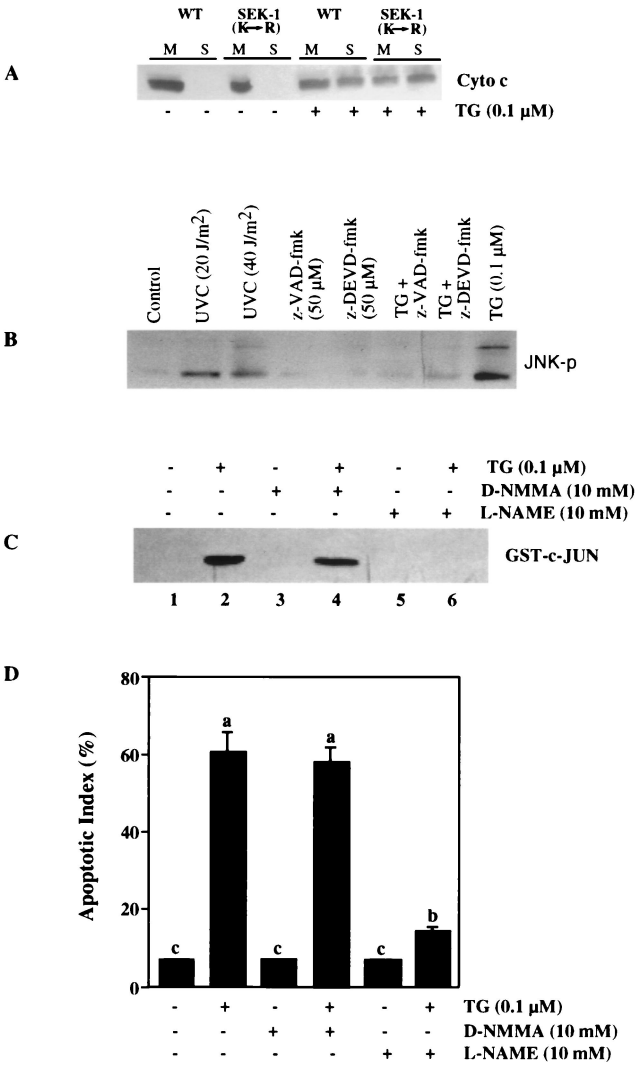

FIG. 11. Mitochondrial events activate JNK and induce apoptosis. (A) A dominant negative mutant SEK1(Lys→Arg) does not inhibit TG-induced cytochrome *c* release from mitochondria to the cytosol. Jurkat cells were plated on 60-mm dishes and transfected with a total of 2 μg of DNA of either empty vector (WT) or mutated SEK1 per ml. After 1 day, cells were incubated with 0.1 μM TG (+) or vehicle (−) for 4 h. Jurkat cells were mechanically lysed and separated into mitochondrial (M) and S100 (S) fractions. The amount of cytochrome *c* present in each fraction was determined by Western blot analysis. (B) Caspase inhibitors block TG-induced JNK activation. Jurkat cells were pretreated with either 50 μM z-VAD-fmk or 50 μM z-DEVD-fmk for 1 h and then subjected to 0.1 μM TG treatment for 4 h. At the end of the culture period, the cells were harvested and lysed and JNK activity was assessed by Western blot analysis with anti-JNK antibody (phosphospecific). Cells were also exposed to UVC (20 or 40 J/m^2) as a positive control. (C) The NOS inhibitor L-NAME, but not D-NMMA (an inactive compound), inhibits TG-induced JNK activation. Jurkat cells were pretreated with either L-NAME (10 mM) or D-NMMA (10 mM) for 45 min and then subjected to 0.1 μM TG treatment for 4 h. JNK activity was measured as described in Materials and Methods. (D) L-NAME, but not D-NMMA, inhibits TG-induced apoptosis. Jurkat cells were pretreated with either L-NAME (10 mM) or D-NMMA (10 mM) for 45 min and then subjected to 0.1 μM TG treatment for 36 h and stained with DAPI. The data are means and standard errors. Significant differences ($P < 0.05$) among groups were determined by analysis of variance with multiple comparisons by the Student-Neuman Keul test and are indicated by different letters. Histograms denoted by a common letter are not significantly different in group comparisons. Means among groups denoted by dissimilar letters are statistically significant.

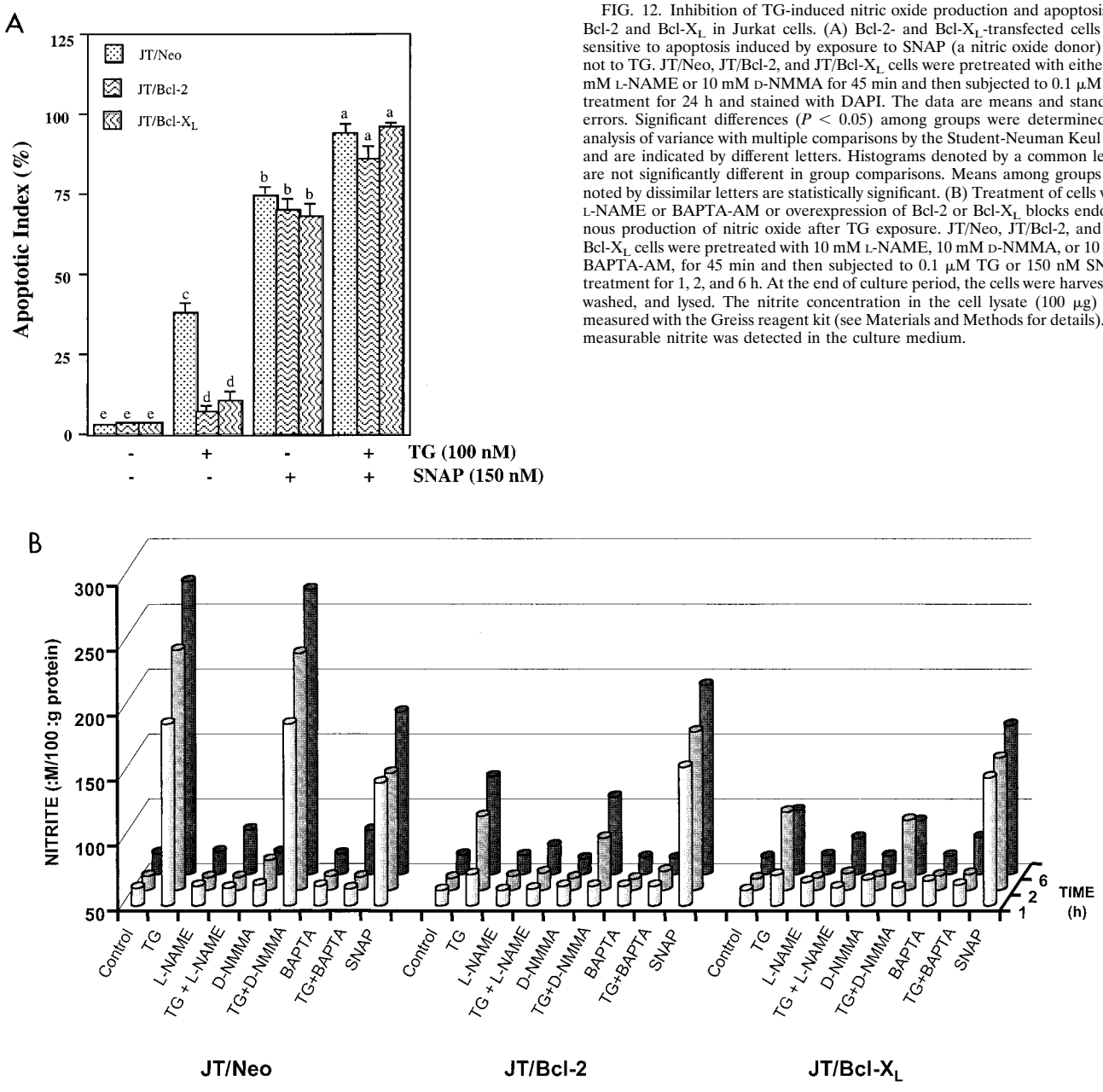

FIG. 12. Inhibition of TG-induced nitric oxide production and apoptosis by Bcl-2 and Bcl-X_L in Jurkat cells. (A) Bcl-2- and Bcl-X_L-transfected cells are sensitive to apoptosis induced by exposure to SNAP (a nitric oxide donor) but not to TG. JT/Neo, JT/Bcl-2, and JT/Bcl-X_L cells were pretreated with either 10 mM L-NAME or 10 mM D-NMMA for 45 min and then subjected to 0.1 μM TG treatment for 24 h and stained with DAPI. The data are means and standard errors. Significant differences ($P < 0.05$) among groups were determined by analysis of variance with multiple comparisons by the Student-Neuman Keul test and are indicated by different letters. Histograms denoted by a common letter are not significantly different in group comparisons. Means among groups denoted by dissimilar letters are statistically significant. (B) Treatment of cells with L-NAME or BAPTA-AM or overexpression of Bcl-2 or Bcl-X_L blocks endogenous production of nitric oxide after TG exposure. JT/Neo, JT/Bcl-2, and JT/Bcl-X_L cells were pretreated with 10 mM L-NAME, 10 mM D-NMMA, or 10 μM BAPTA-AM, for 45 min and then subjected to 0.1 μM TG or 150 nM SNAP treatment for 1, 2, and 6 h. At the end of culture period, the cells were harvested, washed, and lysed. The nitrite concentration in the cell lysate (100 μg) was measured with the Greiss reagent kit (see Materials and Methods for details). No measurable nitrite was detected in the culture medium.

JT/Neo cells. Overexpression of Bcl-2 or Bcl-X_L had no effect on SNAP-induced nitrite production. These results suggest that Bcl-2 and Bcl-X_L can block the calcium-induced endogenous production of nitric oxide by TG and that the prevention of NO generation is the mechanism by which these proteins protect cells from TG-induced apoptosis.

DISCUSSION

In this paper, we demonstrate that TG induces apoptosis through a pathway involving an increase in intracellular calcium levels, generation of nitric oxide, a reduction in mitochondrial membrane potential, release of mitochondrial cytochrome *c*, and activation of caspase-3 and the JNK pathway. We also present evidence that overexpression of Bcl-2 or Bcl-X_L in Jurkat T lymphocytes had no significant effect on the TG-induced mitochondrial and intracellular free calcium levels up to 3 h. The amplitude of intracellular Ca^{2+} transiently induced by TG was not affected by the presence or absence of extracellular Ca^{2+}, indicating that TG must be acting to release intracellular Ca^{2+} stores. The data suggest that apoptosis is a consequence of the increase in calcium level because preventing the increase directly by chelating intracellular calcium prevents apoptosis. TG induces nitric oxide production and JNK activation, both of which precede apoptosis. The JNK activation increases after 2 h of treatment with TG, whereas apoptotic cells begin to appear after 8 h of exposure of the cells to TG. TG-induced activation of the JNK pathway tightly correlates with the subsequent apoptosis in a concentration-dependent manner. In addition, a dominant negative SEK1 mutant can block TG-induced JNK activation and subsequent

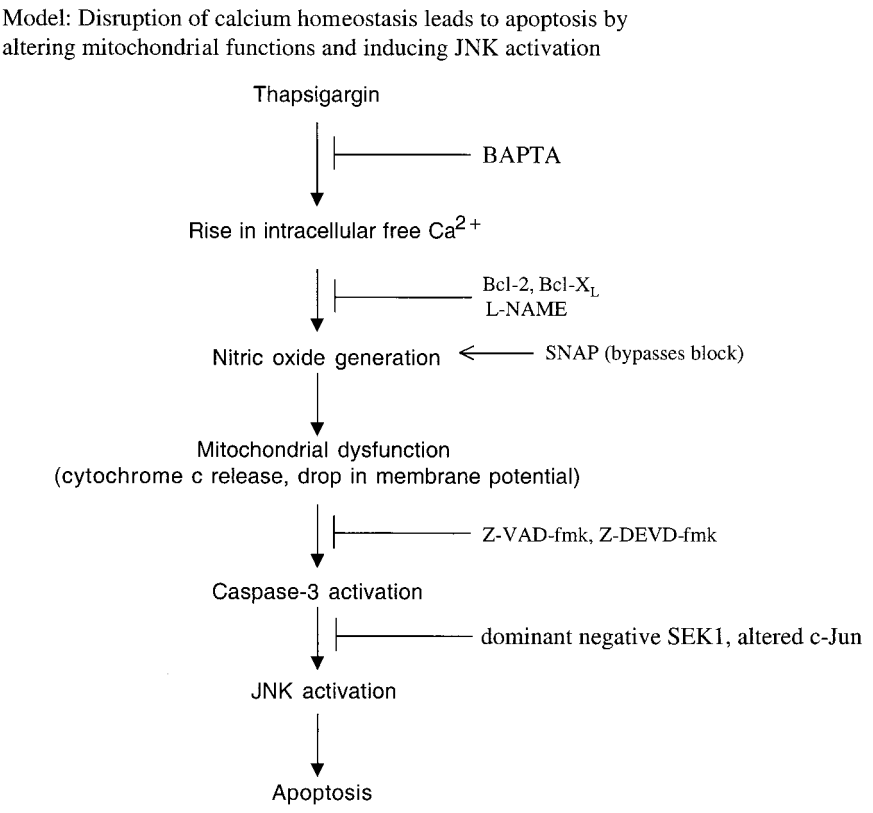

FIG. 13. Model showing that disruption of calcium homeostasis leads to apoptosis by altering mitochondrial functions and inducing JNK activation. Disruption of calcium homeostasis by TG increases the intracellular free calcium level and promotes nitric oxide generation in the mitochondria and loss in mitochondrial membrane potential, leading to cytochrome *c* release, caspase-3 activation, induction of JNK activity, and apoptosis. Overexpression of Bcl-2 or Bcl-X_L has no effect on the transient intracellular calcium levels but inhibits nitric oxide production, reduction in $\Delta\Psi_m$, and cytochrome *c* release, leading to caspase-3 activation and apoptosis.

phosphorylation of c-Jun as well as apoptosis. Consistent with this result, a dominant negative c-Jun mutant, which blocks c-Jun activation, also inhibits apoptotic cell death by TG. Finally, overexpression of Bcl-2 or Bcl-X_L blocks production of nitric oxide, release of cytochrome *c*, reduction in $\Delta\Psi_m$, and activation of caspase-3 and the JNK pathway in Jurkat cells treated with TG. Thus, our data suggest a model by which TG causes increased intracellular Ca^{2+} levels, leading to generation of nitric oxide. The nitric oxide then leads to the release of cytochrome *c* from the mitochondria and a reduction in $\Delta\Psi_m$. The cytochrome *c* results in activation of caspase-3, and caspase-3 activates the JNK pathway, resulting in apoptosis (Fig. 13). Blocking any of the steps, calcium release (BAPTA-AM), nitric oxide production (L-NAME and, for the first time, Bcl-2 and Bcl-X_L), caspase activation (z-VAD-fmk, z-DEVD-fmk), or JNK activation (dominant negative SEK-1 and c-Jun) blocks the TG-induced apoptosis.

In contrast to our findings, it has been reported that Bcl-2 overexpression attenuates the transient Ca^{2+} release in response to TG treatment (19, 31). The ER membrane channel through which Ca^{2+} flows after TG treatment has not been identified but appears to be distinct from the Ca^{2+} release channel associated with the inositol 1,4,5-triphosphate receptor (3, 56). Identification of ion channels associated with the ER membrane may be a requisite for fully understanding the mechanism of action of Bcl-2. He et al. (19) proposed that Bcl-2 may facilitate Ca^{2+} reuptake in the ER by forming pores when the Ca^{2+}-ATPase is inhibited by TG. Since Bcl-2 and Bcl-X_L are also localized to the mitochondrial membrane, mitochondria may play a role in calcium homeostasis (22, 24, 31) and free radical scavenging and antioxidant activity (23, 26, 55, 71). These activities might be cooperative, in light of the relationship between oxidant stress and calcium release leading to apoptosis. In the present study, Bcl-2 and Bcl-X_L overexpression had no effect on mitochondrial and intracellular free calcium levels up to 3 h after TG treatment. However, these proteins affected the generation of nitric oxide as a consequence of calcium release and thereby prevented downstream events including the release of cytochrome *c* from the mitochondria and activation of caspase-3 after TG treatment. If Bcl-2 and Bcl-X_L have an influence on calcium flux, we could not detect it.

Our results indicate that TG induces a persistent activation of the JNK enzyme, which may play a critical role in the apoptotic suicide program. TG strongly stimulates JNK activity after a 4-h exposure of cells, and the kinase activity persists throughout apoptosis. The sustained JNK activation is Ca^{2+} dependent and may serve as a death signal in TG-induced apoptosis. Chelation of intracellular calcium with BAPTA-AM prevented the TG-induced JNK activation and apoptosis, confirming the early mediating role of calcium during TG-induced apoptosis. The lag time between the calcium signal and the activation of JNK is consistent with a role for calcium as an upstream activator of JNK. In agreement with this view, a similar longer stimulation of the JNK enzyme was also observed in some environmental stress-induced forms of apoptosis. For example, exposure of Jurkat cells to lethal doses of γ and UVC radiation rapidly increases JNK activity after 30 min,

and the activation can last at least 12 h without having a significant effect on p38 MAP kinase and ERK activity (6, 7). Withdrawal of NGF from differentiated PC12 neuronal cells results in persistent activation of JNK and p38 MAP kinase with inhibition of ERK activity (69). Although there are variable effects on p38 MAP kinase and ERK activities in different cell systems, the JNK activation is persistent and shows a direct correlation with apoptosis. Furthermore, repression of JNK activation by transfection of a dominant negative mutant, JNK1, prevents γ and UVC irradiation-induced apoptosis (6, 7). Overexpression of a dominant negative mutant of upstream kinase MEK kinase 1 (MEKK1) for JNK inhibits apoptosis induced by deprivation of NGF from differentiated PC12 cells (69). In the present study, transfection of a dominant negative mutant of SEK, an upstream kinase for JNK, also blocks TG-induced apoptosis. All of these observations indicate that sustained JNK activation is essential to induce apoptosis in some types of cell death. The TG-induced persistent JNK activation may be produced by the continued stimulation of upstream activators of the JNK pathway due to cellular damage by ROS or nitric oxide (13). An alternative pathway for prolonged JNK activation by TG may be the inactivation of a dual-specificity phosphatase, an enzyme that can dephosphorylate JNK and ERK, resulting in down-regulation of the activities (35).

Nitric oxide (NO) is an important pleiotropic molecule involved in neurotransmission, regulation of vascular homeostasis, and effector functions of macrophages and endothelial cells (43). NO is derived from the oxidation of L-arginine catalyzed by constitutive (cNOS) or inducible (iNOS) NO synthase. The cytotoxic effects of NO were found to be associated with apoptosis in normal cells (1, 14) and tumor cells (15, 63–65). The mitochondria generate a significant amount of NO, whose production may affect energy metabolism, O_2 consumption, and O_2 free radical formation (16). The activity of mitochondrial NOS is stimulated when Ca^{2+} is taken up by mitochondria (17). In the present study, the activation of JNK is related to the activation of NOS since treatment of cells with the NOS inhibitor L-NAME blocks TG-induced JNK activation and apoptosis.

Bcl-2 is intracellularly located in the places where ROS are generated, such as mitochondria, ER, and nuclear membranes (23). Bcl-2 inhibits ROS-induced apoptosis through regulation of an antioxidation pathway (22, 23). There is a complex interrelationship between oxygen radical damage and intracellular Ca^{2+} fluxes, including evidence that oxidative damage can mobilize Ca^{2+} from intracellular pools located in the ER and mitochondria (46, 50, 72). Therefore, it is interesting to speculate that the effects of Bcl-2 on intracellular Ca^{2+} homeostasis and oxygen radical damage may be related. Reducing Bcl-2 expression with an antisense oligonucleotide increases the sensitivity of the CATH.a cell line to the toxic effects of dopamine (39). Moreover, overexpression of Bcl-2 in PC12 cells can block JNK activation induced by serum deprivation (48). It is not known whether NO plays a role in these systems.

The activation of cysteine proteases from the caspase family appears to be essential for apoptosis to occur (62). These enzymes cleave their substrate(s) after certain recognition sequences ending with an aspartate residue. At least 13 of these enzymes are known, and they seem to cleave with different substrate specificities (62). Recently, it has been shown that activated caspase-3 (activated by genotoxin) can cleave MEKK1 into an active 91-kDa kinase fragment (68). A mutant MEKK1 that is resistant to caspase cleavage can block genotoxin-induced apoptosis (68). In addition, caspase-3-like activity is essential for calphostin c-induced activation of JNK and p38 kinase (47). Similarly in the present study, caspase inhibitors (z-DEVD-fmk and z-VAD-fmk) were able to block TG-induced JNK activity and apoptosis, suggesting the requirement for caspase activity in JNK activation. Moreover, treatment of Jurkat cells with TG resulted in the activation of caspase-3, and this activation was blocked by Bcl-2, Bcl-X_L, or caspase inhibitors.

Alterations in mitochondrial function, in particular the induction of the MPT, are proposed to play a critical role in apoptosis (44). Cytochrome *c* release and mitochondrial membrane depolarization as a result of the opening of permeability transition pores have been proposed as early irreversible events during apoptosis (71). Opening of the MPT pores might mark a point of no return during the effector phase of ongoing apoptosis. Production of nitric oxide in the mitochondria results in mitochondrial lipid degradation and cytochrome *c* release (60, 61, 64). Generation of the nitric oxide may be the important event in the mitochondria for the release of cytochrome *c*, which has been found to activate caspases (28, 29, 70). Consistent with these findings, microinjection of cytochrome *c* results in apoptosis (73) that cannot be inhibited by Bcl-X_L expression (27). In addition, at least one mitochondrial protein (AIF) released following mitochondrial depolarization is an activator of nuclear apoptosis, presumably through caspase activation (59). In a recent report, the induction of the overexpression of Bax in stably transfected Jurkat cells induced MPT, an event that is accompanied by typical features of apoptosis, namely, cytosolic accumulation of cytochrome *c*, caspase activation, cleavage of poly(ADP-ribose) polymerase, DNA fragmentation, and cell death (49). Bcl-2 and Bcl-X_L block apoptosis by preventing cytochrome *c* release to the cytosol, downstream caspase activation, reduction in $\Delta\Psi_m$, and AIF liberation (5, 8, 20, 28, 29, 58, 59, 69). Thus, both the loss of outer mitochondrial membrane integrity leading to cytochrome *c* release and inner membrane depolarization are caspase-activating events that trigger the apoptotic cascade downstream of Bcl-2 and Bcl-X_L.

In conclusion, we have presented data to show that overexpression of Bcl-2 or Bcl-X_L in Jurkat T cells attenuated TG-induced nitric oxide production and apoptosis, a process that requires the activation of caspase-3 and the JNK pathway (Fig. 13). TG-induced apoptosis occurs in a time- and concentration-dependent manner. Corresponding to its proapoptotic action, TG activates the JNK pathway (as indicated by stimulation of JNK and phosphorylation of c-Jun), which occurs before activation of a cell suicide program. A dominant negative mutant SEK1(Lys→Arg) blocks TG-induced JNK activation and subsequent apoptosis. The c-Jun-negative mutant also prevents TG-induced apoptosis. TG-induced apoptosis was caused by a calcium-dependent induction of nitric oxide production. In this system, the antiapoptotic gene products Bcl-2 and Bcl-X_L functioned to prevent apoptosis by blocking the calcium-dependent nitric oxide generation. How these proteins affect NOS activity or expression and whether this mechanism accounts for Bcl-2 and Bcl-X_L effects in other systems are under investigation.

ACKNOWLEDGMENTS

We thank J. Kyriakis for the SEK1(Lys→Arg) vector, Stanley J. Korsmeyer for Bcl-2 and Bcl-X_L expression vectors, and J. Ham for pCDFLAGΔ169 c-Jun. We also extend our thanks to Dr. Charles Filburn for expert assistance and helpful suggestions during the course of the study, as well as to Joe Chrest for help with flow cytometry.

REFERENCES

1. **Albina, J. E., S. Cui, R. B. Mateo, and J. S. Reichner.** 1993. Nitric oxide-mediated apoptosis in murine peritonial macrophages. J. Immunol. **150:** 5080–5085.

2. **Baffy, G., T. Miyashita, J. R. Williamson, and J. C. Reed.** 1993. Apoptosis induced by withdrawal of interleukin-3 (IL-3) from an IL-3-dependent hematopoietic cell line is associated with repartitioning of intracellular calcium and is blocked by enforced Bcl-2 oncoprotein production. J. Biol. Chem. **268:**6511–6519.
3. **Bansal, V. S., and P. W. Majerus.** 1990. Phosphatidylinositol-derived precursors and signals. Annu. Rev. Cell Biol. **6:**41–67.
4. **Bernardi, P., K. M. Broekemeier, and D. R. Pfeiffer.** 1994. Recent progress on regulation of the mitochondrial permeability transition pore; a cyclosporin-sensitive pore in the inner mitochondrial membrane. J. Bioenerg. Biomembr. **26:**509–517.
5. **Boise, L. H., M. Gonzalez-Garcia, C. E. Postema, L. Ding, T. Lindsten, L. A. Turka, X. Mao, G. Nunez, and C. B. Thompson.** 1993. Bcl-X, a bcl-2 related gene that functions as a dominant regulator of apoptotic cell death. Cell **74:**597–608.
6. **Chen, Y.-R., C. F. Meyer, and T.-H. Tan.** 1996. Persistent activation of c-Jun N-terminal kinase 1 (JNK1) in radiation-induced apoptosis. J. Biol. Chem. **271:**631–634.
7. **Chen, Y.-R., X. Wang, D. Templeton, R. Davis, and T.-H. Tan.** 1996. The role of c-Jun N-terminal kinase (JNK) in apoptosis induced by ultraviolet C and radiation. J. Biol. Chem. **271:**31929–31936.
8. **Chinnaiyan, A. M., K. Orth, K. O'Rourke, H. Duan, G. G. Poirier, and V. M. Dixit.** 1996. Molecular ordering of the cell death pathway: Bcl-2 and Bcl-X_L function upstream of the CED-3-like apoptotic proteases. J. Biol. Chem. **271:**4573–4576.
9. **Chlichlia K, M. E. Peter, M. Rocha, C. Scaffidi, M. Bucur, P. H. Krammer, V. Schirrmacher, and V. Umansky.** 1998. Caspase activation is required for nitric oxide-mediated, CD95(APO-1/Fas)-dependent and independent apoptosis in human neoplastic lymphoid cells. Blood **91:**4311–4320.
10. **Cohen, G. M., X.-M. Sun, R. T. Snowden, M. G. Ormerod, and D. Dinsdale.** 1993. Identification of a transitional preapoptotic population of thymocytes. J. Immunol. **151:**566–574.
11. **Dérijard, B., J. Raingeaud, T. Barrett, I.-H. Wu, J. Han, R. Ulevitch, and R. Davis.** 1995. Independent human MAP-kinase signal transduction pathways defined by MEK and MKK isoforms. Science **267:**682–685.
12. **Dérijard, B., M. Hibi, I.-H. Wu, T. Barret, B. Su, T. Deng, M. Karin, and R. Davis.** 1994. JNK1: a protein kinase stimulated by UV light and Ha-Ras that binds and phosphorylates the c-Jun activation domain. Cell **76:**1025–1037.
13. **Ernster, L., and G. Schatz.** 1981. Mitochondria: a historical review. J. Cell Biol. **91:**227–255.
14. **Fehsel, K., K.-D. Krsncke, K. L. Meyer, H. Huber, V. Wahn, and V. Kolb-Bachofen.** 1995. Nitric oxide induces apoptosis in mouse thymocytes. J. Immunol. **155:**2858–2862.
15. **Geng, Y.-J., K. Hellstrand, A. Wennmalm, and G. K. Hansson.** 1996. Apoptotic death of human leukemic cells induced by vascular cells expressing nitric oxide synthase in response to γ-interferon and tumor necrosis factor-α. Cancer Res. **56:**866–871.
16. **Giulivi, C., J. J. Poderosa, and A. Boveris.** 1998. Production of nitric oxide by mitochondria. J. Biol. Chem. **273:**11038–11043.
17. **Ghafourifar, P., and C. Richter.** 1997. Nitric oxide synthase activity in mitochondria. FEBS Lett. **418:**291–296.
18. **Ham, J., C. Babij, J. Whitfield, C. Pfarr, D. Lallemand, M. Yaniv, and L. Rubin.** 1995. A c-Jun dominant negative mutant protects sympathetic neurons against programmed cell death. Neuron **14:**927–939.
19. **He, H., M. Lam, T. S. McCormic, and C. W. Distelhorst.** 1997. Maintenance of calcium homeostasis in the endoplasmic reticulum by Bcl-2. J. Cell Biol. **138:**1219–1228.
20. **Heiden, M. G. V., N. S. Chandel, E. K. Williamson, P. T. Schumacker, and C. B. Thompson.** 1997. Bcl-X_L regulates the membrane potential and volume homeostasis of mitochondria. Cell **91:**627–637.
21. **Hirai, S., R. Ryseck, F. Mechta, R. Bravo, and M. Yaniv.** 1989. Characterization of Jun D: a new member of the jun proto-oncogene family. EMBO J. **8:**1433–1439.
22. **Hockenbery, D.** 1995. Defining apoptosis. Am. J. Pathol. **146:**16–19.
23. **Hockenbery, D., Z. Oltvai, X.-M. Yin, C. Milliman, and S. Korsmeyer.** 1993. Bcl-2 functions in an antioxidant pathway to prevent apoptosis. Cell **75:**241–251.
24. **Ichas, F., L. S. Jouaville, and J.-P. Mazat.** 1997. Mitochondria are excitable organelles capable of generating and conveying electrical and calcium signals. Cell **89:**1145–1153.
25. **Ichijo, H., E. Nishida, K. Irie, P. Dijke, M. Saitoh, T. Moriguchi, M. Takagi, K. Matsumoto, K. Miyazono, and Y. Gotoh.** 1997. Induction of apoptosis by ASK1, a mammalian MAPKKK that activates SAPK/JNK and p38 signaling pathways. Science **275:**90–94.
26. **Kane, D. J., T. A. Sarafian, R. Anton, H. Hahn, E. B. Gralla, J. S. Valentine, T. Ord, and D. E. Bredesen.** 1994. Bcl-2 inhibition of neural death: decreased generation of reactive oxygen species. Science **262:**1274–1277.
27. **Kharbanda, S., P. Pandey, L. Schofield, S. Israels, R. Roncinske, K. Yoshida, A. Bharti, Z.-M. Uuan, S. Saxena, R. Weichselbaum, C. Nalin, and D. Kufe.** 1997. Role of Bcl-X_L as an inhibitor of cytosolic cytochrome c accumulation in DNA damage-induced apoptosis. Proc. Natl. Acad. Sci. USA **94:**6939–6942.
28. **Kim, C. N., H. Wang, Y. Huang, A. M. Ibrado, L. Liu, G. Fang, and K. Bhalla.** 1997. Overexpression of Bcl-X_L inhibits ara-C-induced mitochondrial loss of cytochrome c and other perturbations that activate the molecular cascade of apoptosis. Cancer Res. **57:**3115–3120.
29. **Kluck, R. M., E. Bossy-Wetzel, D. R. Green, and D. D. Newmeyer.** 1997. The release of cytochrome c from mitochondria: a primary site for Bcl-2 regulation of apoptosis. Science **275:**1132–1136.
30. **Kyriakis, J., P. Banerjee, E. Nikolakaki, T. Dai, E. Rubie, M. Ahmad, J. Avruch, and J. Woodgett.** 1994. The stress-activated protein kinase subfamily of c-Jun kinases. Nature **369:**156–160.
31. **Lam, M., M. B. Bhat, G. Nunez, J. Ma, and C. W. Distelhorst.** 1998. Regulation of Bcl-xl channel activity by calcium. J. Biol. Chem. **273:**17307–17310.
32. **Lam, M., G. Dubyak, L. Chen, G. Nunez, R. L. Miesfeld, and C. W. Distelhorst.** 1994. Evidence that Bcl-2 represses apoptosis by regulating endoplasmic reticulum-associated Ca^{2+} fluxes. Proc. Natl. Acad. Sci. USA **91:**6569–6573.
33. **Lam, M., M. B. Bhat, G. Nuñez, J. Ma, and C. W. Distelhorst.** 1998. Regulation of Bcl-X_L channel activity by calcium. J. Biol. Chem. **273:**17307–17310.
34. **Liu, X., C. N. Kim, J. Yang, R. Jemmerson, and X. Wang.** 1996. Induction of apoptotic program in cell-free extracts: requirement for dATP and cytochrome c. Cell **86:**147–157.
35. **Liu, Y., M. Gorospe, C. Yang, and N. J. Holbrook.** 1995. Role of mitogen-activated protein kinase phosphatase during the cellular response to genotoxic stress. J. Biol. Chem. **270:**8377–8380.
36. **Luo, Y., H. Umegaki, X. Wang, R. Abe, and G. S. Roth.** 1998. Dopamine induces apoptosis through an oxidation-involved SAPK/JNK activation pathway. J. Biol. Chem. **273:**3756–3764.
37. **Magnelli, L., M. Cinelli, A. Turchetti, and V. P. Chiarugi.** 1994. Bcl-2 overexpression abolishes early calcium waving preceding apoptosis in NIH-3T3 murine fibroblasts. Biochem. Biophys. Res. Commun. **204:**84–90.
38. **Marin, M. C., A. Fernandez, R. J. Bick, S. Brisbay, L. M. Buja, M. Snuggs, D. J. McConkey, A. C. von Eschenbach, M. J. Keating, and T. J. McDonnell.** 1996. Apoptosis suppression by bcl-2 is correlated with the regulation of nuclear and cytosolic Ca^{2+}. Oncogene **12:**2259–2266.
39. **Masserano, J. M., L. Gong, H. Kulaga, I. Baker, and R. J. Wyatt.** 1996. Dopamine induces apoptotic cell death of a catecholaminergic cell line derived from the central nervous system. Mol. Pharmacol. **50:**1309–1315.
40. **Minn, A. J., P. Velez, S. L. Schendel, H. Liang, S. W. Muchmore, S. W. Fesik, M. Fill, and C. B. Thompson.** 1997. Bcl-X_L forms an ion channel in synthetic lipid membranes. Nature (London) **385:**353–357.
41. **Muchmore, S. W., M. Sattler, H. Liang, R. P. Meadows, J. E. Harlan, H. S. Yoon, D. Nettesheim, B. S. Chang, C. B. Thompson, S.-L. Wong, S. C. Ng, and S. W. Fesik.** 1996. X-ray and NMR structure of human Bcl-X_L, an inhibitor of programmed cell death. Nature (London) **381:**335–341.
42. **Murphy, A. N., D. E. Bredesen, G. Cortopassi, E. Wang, and G. Fiskum.** 1996. Bcl-2 potentiates the maximal calcium uptake capacity of neural cell mitochondria. Proc. Natl. Acad. Sci. (USA) **93:**9893–9898.
43. **Nathan, C. F., and Q.-W. Xie.** 1994. Nitric oxide synthase: rolles, tolls, and controls. Cell **78:**915–922.
44. **Nieminen, A. L., A. K. Saylor, S. A. Tesfai, B. Herman, and J. J. Lemasters.** 1995. Contribution of the mitochondrial permeability transition to lethal injury after exposure of hepatocytes to t-butylhydroperoxide. Biochem. J. **307:**99–106.
45. **Oltvai, Z. N., and S. J. Korsmeyer.** 1994. Checkpoints of dueling dimers foil death wishes. Cell **79:**189–192.
46. **Orrenius, S., M. J. Burkitt, G. E. N. Kass, J. M. Dypbukt, and P. Nicotera.** 1992. Calcium ions and oxidative cell injury. Ann. Neurol. **32:**S33–S42.
47. **Ozaki, I., E. Tani, H. Ikemoto, H. Kitagawa, and H. Fujikawa.** 1999. Activation of stress-activated protein kinase/c-Jun NH2-terminal kinase and p38 kinase in calphostin C-induced apoptosis requires caspase-3-like proteases but is dispensable for cell death. J. Biol. Chem. **274:**5310–5317.
48. **Park, D. S., L. Stefanis, C. Y. I. Yan, S. E. Farinelli, and L. A. Greene.** 1996. Ordering the cell death pathway. J. Biol. Chem. **271:**21898–21905.
49. **Pastorino, J. G., S.-T. Chen, M. Tafani, J. W. Snyder, and J. F. Farber.** 1998. The overexpression of Bax produces cell death upon induction of the mitochondrial permeability transition. J. Biol. Chem. **273:**7770–7775.
50. **Reed, D. J.** 1990. Review of the current status of calcium and thiols in cellular injury. Chem. Res. Toxicol. **3:**495–502.
51. **Reed, J. C.** 1997. Double identity for proteins of the Bcl-2 family. Nature **387:**773–776.
52. **Reed, J. C.** 1997. Cytochrome c: can't live with it—can't live without it. Cell **91:**559–562.
53. **Reed, J. C.** 1994. Bcl-2 and the regulation of programmed cell death. J. Cell Biol. **124:**1–6.
54. **Rabinovitch, P. S., C. H. June, A. Grossman, and J. A. Ledbetter.** 1986. Heterogeneity among T cells in intracellular free calcium responses after mitogen stimulation with PHA or anti-CD3. Simultaneous use of Indo-1 and immunofluorescence with flow cytometry. J. Immunol. **137:**952–961.
55. **Richter, C.** 1993. Pro-oxidants and mitochondrial Ca^{2+}: their relationship to apoptosis and oncogenesis. FEBS Lett. **325:**104–107.
56. **Rizzuto, R., C. Bastianutto, M. Brini, M. Murgia, and T. Pozzan.** 1994.

Mitochondrial Ca^{2+} homeostasis in intact cells. J. Cell Biol. **126:**1183–1194.
57. **Sambrook, J. F.** 1990. The involvement of calcium in transport of secretary proteins from the endoplasmic reticulum. Cell **61:**197–199.
58. **Srivastava, R. K., A. R. Srivastava, S. J. Korsmeyer, M. Nesterova, Y. S. Cho-Chung, and D. L. Longo.** 1998. Involvement of microtubules in the regulation of Bcl2 phosphorylation and apoptosis through cyclic AMP-dependent protein kinase. Mol. Cell. Biol. **18:**3509–3517.
59. **Susin, S. A., N. Zamzami, M. Castedo, T. Hirsch, P. Marchetti, A. Macho, E. Daugas, M. Geuskens, and G. Kroemer.** 1996. Bcl-2 inhibits the mitochondrial release of an apoptotic protease. J. Exp. Med. **184:**1331–1341.
60. **Susin, S. A., N. Zamzami, M. Castedo, E. Daugas, H. G. Wang, S. Geley, F. Fassy, J. C. Reed, and G. Kroemer.** 1997. The central execution of apoptosis: multiple connections between protease activation and mitochondria in Fas/APO-1/CD95- and ceramide-induced apoptosis. J. Exp. Med. **186:**25–37.
61. **Thompson, C. B.** 1995. Apoptosis in the pathogenesis and treatment of disease. Science **267:**1456.
62. **Thornberry, N. A., and Y. Lazebnik.** 1998. Caspases: enemies within. Science **281:**1312–1316.
63. **Uehara, T., Y. Kikuchi, and Y. Nomura.** 1999. Caspase activation accompanying cytochrome c release from mitochondria is possibly involved in nitric oxide-induced neuronal apoptosis in SH-SY5Y cells. J. Neurochem. **72:**196–205.
64. **Ushmorov A., F. Ratter, V. Lehmann, W. Droge, V. Schirrmacher, and V. Umansky.** 1999. Nitric oxide-induced apoptosis in human leukemic lines requires mitochondrial lipid degradation and cytochrome C release. Blood **93:**2342–2352.
65. **Umansky, V., M. Bucur, V. Schirrmacher, and M. Rocha.** 1997. Activated endothelia cells induce apoptosis in lymphoma cells: role of nitric oxide. Int. J. Oncol. **3:**1043–1050.
66. **Vavssiäre, J.-L, P. X. Petit, Y. Risler, and B. Mignotte.** 1994. Commitment to apoptosis is associated with changes in mitochondrial biogenesis and activity in cell lines conditionally immortalized with simian virus 40. Proc. Natl. Acad. Sci. USA **91:**11752–11756.
67. **Verheij, M., R. Bose, X. Lin, B. Yao, W. Jarvis, S. Grant, M. Birrer, E. Szabo, L. Zon, J. Kyriakis, A. Haimovitz-Friedman, Z. Fuks, and R. Kolesnick.** 1996. Requirement for ceramide-initiated SAPK/JNK signalling in stress-induced apoptosis. Nature **380:**75–79.
68. **Widmann C., P. Gerwins, N. L. Johnson, M. B. Jarpe, and G. L. Johnson.** 1998. MEK kinase 1, a substrate for DEVD-directed caspases, is involved in genotoxin-induced apoptosis. Mol. Cell. Biol. **18:**2416–2429.
69. **Xia, Z., M. Dickens, J. Raingeaud, R. Davis, and M. Greenberg.** 1995. Opposing effects of ERK and JNK-p38 MAP kinases on apoptosis. Science **270:**1326–1331.
70. **Yang, J., X. Liu, K. Bhalla, C. N. Kim, A. M. Ibrado, J. Cai, T.-I. Peng, D. P. Jones, and X. Wang.** 1997. Prevention of apoptosis by Bcl-2: release of cytochrome c from mitochondria blocked. Science **275:**1126–1132.
71. **Zamzami N., P. Marchetti, M. Castedo, D. Decaudin, A. Macho, T. Hirsch, S. A. Susin, P. X. Petit, B. Mignotte, and G. Kroemer.** 1995. Sequential reduction of mitochondrial transmembrane potential and generation of reactive oxygen species in early programmed cell death. J. Exp. Med. **182:**367–377.
72. **Zhang, Y., O. Marcillat, C. Giulivi, L. Ernster, and K. J. A. Davies.** 1990. The oxidative inactivation of mitochondrial electron transport chain components and ATPase. J. Biol. Chem. **265:**16330–16336.
73. **Zhivotovsky, B., S. Orrenius, O. T. Brustugun, and S. O. Døskeland.** 1998. Injected cytochrome c induces apoptosis. Nature (London) **391:**449–450.